This is to certify that the

dissertation entitled

Computer Simulation Studies of Ion Trajectories in Triple Quadrupole Mass Spectrometry

presented by

Jiin-Wu Chai

has been accepted towards fulfillment
of the requirements for

Ph.D. degree in Chemistry

C G Enke

Major professor

Date 3/19/82

COMPUTER SIMULATION STUDIES OF ION TRAJECTORIES IN TRIPLE QUADRUPOLE MASS SPECTROMETRY

By

Jiin-Wu Chai

A DISSERTATION

Submitted to

Michigan State University

in partial fulfillment of the requirements

for the degree of

DOCTOR OF PHILOSOPHY

Department of Chemistry

1982

ABSTRACT

COMPUTER SIMULATION STUDIES OF ION TRAJECTORIES
IN TRIPLE QUADRUPOLE MASS SPECTROMETRY

By

Jiin-Wu Chai

Computer simulation methodology has been used to study ion trajectories in triple quadrupole mass spectrometry (TQMS), focusing on three main components: the RF-only quadrupole, the ion source, and the lens system.

Results from the study of the RF-only quadrupole show that the applied RF voltage, the frequency, the quadrupole cross section, and the ratio of the radius of the rods to the half length of their separation all affect both the low mass limit and the high mass limit of transmission through the quadrupole. The other significant factors studied which affect the characteristics of the quadrupole include the ion's off-axis energy, the quadrupole length, the exit orifice, the radial angle of ion path on the cross section of the quadrupole, the phase of quadrupole radio frequency voltage at the time of ion entry, the axial energy, the ion fragmentation, and the time of its fragmentation. Several recommendations for TQMS users to maximize the ratio of the

high mass limit to the low mass limit and several guidelines for instrumentation, operation, and applications of the RF-only quadrupole are given.

Four new types of ion sources for an electron impact mass spectrometer have been designed and their performance has been studied. They will produce focused ion current three thousand times higher than that produced by conventional ion sources. A high efficiency ion source has been designed to produce ions of very small kinetic energy spread. The use of such sources would significantly increase the sensitivity of quadrupole mass spectrometers.

The effect and selection of instrumentation and operation parameters for lens systems have been studied. Three types of ion path benders have been designed to eliminate the interference of accelerated neutral molecules in TQMS. An inter-quadrupole lens system has been designed and has increased the transmission of high mass ions in quadrupole mass spectrometry.

To My Parents, My Wife, and

My Family

ACKNOWLEDGMENTS

Thank God. God provides all. All are of Him by His Love.

The greatest gratitude I owe to my dear parents for their everlasting love which consists of whole-hearted support, enormous sacrifices, tender guidance, provision of needs, and faith and hope that never fail.

Many thanks to Professor Christie G. Enke for his excellent guidance so that this research could be accomplished. I will always appreciate his kindness, encouragement, wide support, and help.

I am grateful to my guidance committee at Michigan State University, including Drs. Andrew Timnick, William Reusch, Richard H. Schwendeman. I especially thank professor Andrew Timnick for serving as the second reader and for his kindness and help. I would like to express my thanks to Professors Richard H. Schwendeman and William Reusch for valuable discussions. Professor Donald G. Farnum is appreciated for serving on my guidance committee during Dr. Reusch's sabbatical and for his help.

I would like to acknowledge Dr. Thomas Atkinson for his help and valuable suggestions in the computer programming. "Tom" is always sharing and willing to help. Thank also Dr. Richard Alan Yost for sharing the original program.

I am thankful to Professor Charles C. Sweeley for the generous sharing of his personal library. Thanks are due to the Department of Biochemistry at MSU for opportunity given to me to do some experiments on GC/MS/DS instruments and GC column preparations. I would like to express my appreciation to Dr. Paul W. W. Hunter for his kindness, help, and friendship. Thanks also to Drs. George E. Leroi, John Allison, and Paul Hunt for valuable discussions.

The support from the Department of Chemistry at MSU with teaching assistantships is highly appreciated. The supports of research assistantships from the Office of Naval Research, and the National Institute of Health are also appreciated.

The sharing and communication among the members of the C. G. Enke Company research group were helpful. Especially, I thank Hugh Gregg and Meg McFarland for valuable suggestions. Thanks also to Ching-Cherng Lii, Shechoing Lin, Kaz Latven, John Chakel, Phil Hoffman, Pete Aiello, and other colleagues in the "mass spec subgroup" for discussions.

I appreciate the brothers and sisters in the MSU Chinese Christian Fellowship for their many expressions of concern, prayer, and assistance.

My family overwhelms me with their love. My sister A-Su has always played a very important role to help and support me and share my burden. My sister Yuh-Hua and her

family have provided much concern, support, and help. My brother-in-law Chan-Wo Chang and his family bore my duties at home. I am also grateful to my brother Jiin-Wen, my sister Yuh-Chyu and her family, and other members for their help. I am thankful to my parents-in-law and the families of my wife's sisters and brothers for their kindness and help. Our son Shua helps with his patience. My wife, Lien-na, with everlasting love, helped me to succeed in this research. Her spiritual support is so important especially at the toughest moments. She does her best with our family needs, takes good care of our son, and has provided invaluable assistance in the editing and typing of this dissertation.

TABLE OF CONTENTS

LIST OF TABLES

LIST OF FIGURES

CHAPTER 1

INTRODUCTION

This dissertation is a description of computer simulation studies of ion trajectories in triple quadrupole mass spectrometry (TQMS). The TQMS instrument developed in our laboratory has introduced a new dimension to mass spectrometry [1-5]. It is impossible to observe directly the ion trajectories in TQMS and it is difficult to test new possible designs by trial-and-error modification of the instrument. Computer simulation studies afford a fast and effective tool to understand the behavior of ions in TQMS and to examine the characteristics of new designs. In this research, a computer simulation method provides an important way to investigate the characteristics of significant components in TQMS and to develop new designs for instrument improvements and advanced applications. The investigations and developments in this study include the RF-only quadrupole chamber, the ion source, and the lens system.

Organization of this Dissertation

This dissertation consists of six chapters. This chapter introduces the thesis topics and the goals and methods used in this research. Also included are a brief

description of the significance of this research, brief descriptions of succeeding chapters, arguments on the validity of the ion trajectory simulation program, and the basic principles of the present work.

The second chapter presents a detailed investigation of ion trajectories in the RF-only quadrupole chamber. The role of computer simulation study of this chamber is followed by a historical review of studies on quadrupole filters by computer calculations, and by a comparison of previous work with the present work. A previous study of the validity of this program's simulation results, the criteria of setting up the quadrupole filter, the procedures of simulation experiments, and the range of experimental values are described. Variables which determine the performance of the quadrupole are investigated, their results are presented and discussion follows. These variables include the applied RF voltage, the frequency, the quadrupole cross section, ion's off-axis energy, the ratio of the radius of the rods to the half length of their separation, the quadrupole length, the diameter of the exit orifice, the radial angle of ion path on the plane surface perpendicular to the axis, the phase of quadrupole radio frequency at the time of ion entry, the ion fragmentation after collision in the chamber, and the time of its fragmentation. This chapter not only provides equations based on these results, but also provides suggestions and

guidelines for analytical instrumentation, operation, and application.

Chapter 3 provides a historical review of ion source design and the simulation study of the electron impact (EI) ion source system first used in our mass spectrometer. The reasons for the poor efficiency of that source have been presented. The performances of ten other possible ion source designs have been compared theoretically with that of the original design. The basis for the superiority of these new designs over the old one have been explained. Four new types of EI source designs have been studied in detail by computer simulation. Theoretical predictions of their efficiencies have been tabulated and compared. Methods for their construction have been suggested. A new ion source has been designed to produce ions of small kinetic energy spread. Ion residence time in this source and the kinetic energy distribution of ions at the chamber exit have been presented.

Computer-aided studies of lens systems in mass spectrometry have been described in Chapter 4. An inter-quadrupole lens system and three types of ion path bender designs in TQMS have been presented. The parameters of interest include the aperture, the thickness, and the angle of each lens, and the distance between adjacent lenses or between the lens and the ion source chamber. The effect of operation parameters for each lens element and the

selection of them have been studied. In the conclusion section, some major considerations in operation and design of the lens systems are pointed out.

Chapter 5 describes the computer simulation program used in this research. The origin, the modification, the validity, and the contents of the program have been described. The function of each part of the program has been discussed. Following that, the concept, operation, time resolution, and outcome of the program are presented.

The final chapter includes a statement of conclusions, recommendations for future research in mass spectrometry by computer simulation, suggestions for improvement of the simulation work, and some prospects for future research.

Basic Principles of this Work

This research uses the computer to calculate ion trajectories under the effect of an electric field. The PDP 11/40 minicomputer with RSX-11M multiuser operating system is used. The computer program, which uses digital simulation, is written in Fortran IV. This program has been used to calculate ion trajectories in the triple quadrupole mass spectrometer [4]. The good success of this program in a comparison of its simulated trajectories with experiment and theory is described in the next chapter.

The program can set up the electrodes with the desired configuration in two dimensions. The size of each dimension can be adjusted according to the need for accuracy and within the limit of memory size and then the electric field can be "built". The potential between positive and negative electrodes is Φ_0, the potential at any point in the quadrupole is given by quadrupole theory [6] as

$$\Phi = \frac{\Phi_0 (x^2 - y^2)}{2r_0^2} \qquad (1\text{-}1)$$

where x and y are the Cartesian coordinates, and $2r_0$ is the minimum distance between opposite electrodes. The acceleration force acting on a particle in this field is given by the elementary equations in classical physics:

$$F = eE = ma \qquad (1\text{-}2)$$

where F is the force, m is the mass of the ion, a is the acceleration, e is the electronic charge, and E is the electric field. The force in the x-direction is then

$$F_x = ma_x = eE_x = -e\frac{\partial \Phi(x, y, z)}{\partial x} = -e\frac{\partial \Phi(x)}{\partial x} \qquad (1\text{-}3)$$

The equations of motion are

$$\frac{d^2x}{dt^2} + \frac{2e}{mr_0^2}\Phi_0 x = 0 \qquad (1\text{-}4)$$

$$\frac{d^2y}{dt^2} - \frac{2e}{mr_0^2}\Phi_0 y = 0 \qquad (1\text{-}5)$$

$$\frac{d^2z}{dt^2} = 0 \qquad (1\text{-}6)$$

where t is time. The equations of motion can be expressed as

$$\frac{d^2x}{dt^2} + \frac{2e}{mr_0^2}(U + V\cos\omega t)x = 0 \qquad (1\text{-}7)$$

$$\frac{d^2y}{dt^2} - \frac{2e}{mr_0^2}(U + V\cos\omega t)y = 0 \qquad (1\text{-}8)$$

$$\frac{d^2z}{dt^2} = 0 \qquad (1\text{-}9)$$

where U is the direct current (DC) voltage, V is the peak RF voltage, and ω is the angular frequency $2\pi f$.

A simple kinetic energy equation $KE = 0.5\ mv^2$ is used, where KE is the kinetic energy, and v is the velocity. Simple trigonometric functions of sine, cosine, and tangent are used. The voltage, frequency, mass to charge ratio (m/z), position, and energy of the ion can be chosen by the user before running the program.

As the simulation begins, the electric field produces an acceleration force on the ion of m/z. For a very brief time, the acceleration can be considered constant. The energy, the direction and the position of this ion are then calculated after a selected time interval. In the RF-only quadrupole field, the time interval used is one hundredth of the period of the RF field. In succeeding computation cycles, the new acceleration force, velocity, direction, position, and energy are then calculated for each succeeding interval of time.

Ion trajectories can be plotted on the Tektronix graphics terminal for direct observation, or on the Printronix graphics printer or the Versatec graphics printer for hard copy. The final position, energy, direction, and traveling time are printed on the CRT terminal. This provides effective interaction and communication between the user and the computer for efficient experimentation.

CHAPTER 2

COMPUTER SIMULATION OF AN RF-ONLY QUADRUPOLE CHAMBER IN TRIPLE QUADRUPOLE MASS SPECTROMETRY

Introduction

This chapter describes computer simulation studies of ion trajectories in an RF-only quadrupole chamber in TQMS . TQMS [1-3] has expanded the potential areas of application for mass spectrometry. This new technique incorporates a high efficiency collision activated dissociation process [4], which facilitates fragmentation pathway studies, direct mixture analysis, and structure elucidation [2,5]. The RF-only quadrupole is the central part of TQMS; therefore its characteristics as the collision activated decomposition chamber are important. Computer simulation studies provide a powerful way to explore quadrupole system behavior with the advantages of high speed, low cost, and relative simplicity in testing the effects of design variations.

Computer simulation methods have been used by several researchers to study quadrupole devices in the mass filter mode. Dawson [6] presented a thorough review of the calculations of ion trajectories up to 1975. He and Meunier [7] studied some distortions in quadrupole fields and their relation to mass filter performance. They studied the

problem of field imperfection and concluded with a suggestion for quadrupole mass filter construction by correcting the errors of positioning.

McGilvery and Morrison [8] designed and constructed a tandem quadrupole mass spectrometer for the study of ion photodissociation processes. They also used a computer simulation method to study ion trajectories, ion distributions and ion densities in their system. Ghosh and Arora [9] calculated mass peak shapes and resolution in quadrupole mass filters. They presented beam injection conditions for optimum resolution on a scan line.

Campana and Jurs [10] used numerical computation to simulate ion trajectories in an ideal quadrupole field. They compared numerical integration techniques and matrix methods. They presented the investigation and the results of ion exit distributions with the aid of computer graphics. Dawson [11] studied energetics of ions in quadrupole fields with the phase-space dynamics approach. He concluded that this approach is a simple, exact method of characterizing ion kinetic energy distributions in quadrupole fields. He again used this approach to study problems of ion optical design for the quadrupole mass filter [12]. Algebraic relationships were tabulated for both x and y directions for the full quadrupole field and for linear fringing fields of one, two and three RF cycles. Arora, Agarwal and Ghosh [13] studied ion transmission factors in quadrupole mass filters.

They also presented sensitivities for a complete range of ion beam injection conditions from parallel to totally diverging beams.

Bonner, Hamilton and March [14] calculated the phase-space parameters for quadrupole devices. They concluded that their method is both fast and accurate. Richards and McLellan [15] presented a fast computer simulation of a quadrupole mass filter driven by a sinusoidal RF waveform. They showed time savings of factors of 10 or more.

Dawson [16] studied the performance of the quadrupole mass filter with separated RF and DC fringing fields. He reported that there is a good agreement between theoretical predictions and experimental measurements for the studies of the separated RF and DC fringing fields. In another paper [17], he also showed experimental measurements of quadrupole mass analyser performance and comparison with theoretical predictions. He concluded that the measured characteristics are in reasonable accord with his calculations based on phase-space dynamics. Hennequin and Inglebert [18] presented an experimental study on the acceptance of a quadrupole mass filter. They concluded that their experimental results were in a good agreement with Dawson's theoretical calculations.

One of the recent studies concerned the effects of the variables on ion trajectories in the RF-only quadrupole [4]

using the program developed by McGilvery and Morrison [8]. These variables included the RF peak voltage, the RF frequency, the pole diameter of the quadrupole, the ion's off-axis energy and its mass. The orbit period, the orbit length, the average velocity, the low mass limit, and the high mass limit were studied by this simulation program and presented in equations expressing the relationships among those variables. Some experiments were performed to test the validity of this simulation program. The transmission of ions of m/z value 15, 28, and 41 from cyclohexane were measurred as a function of peak RF voltage. An experimental value of 0.4 was obtained for the constant term in the expression $Ml = V/F^2d^2$ for the low mass limit. This compares with the simulation study result of 0.5. The orbit period was reported experimentally to obey the relationship $\tau = (7x10^{-6}mfd^2)/v$ which is quite close to the equation from simulation $\tau = (6x10^{-6}mfd^2)/v$, and the theoretical expression $\tau = (7.5x10^{-6}mfd^2)/v$. [6]. Such good agreement among experiment, simulation, and theory supports the validity of using this program for accurate computer simulation of ion trajectories in the RF-only only quadrupole.

In the present work, the computer simulation method is used to further investigate the effects of the RF peak voltage, frequency, the quadrupole cross section, the ion's off-axis energy, and several other factors on the

performance of the RF-only quadrupole. This study presents equations for the low mass limit and the high mass limit with additional consideration of the effect of the ratio of the electrode radius to the half length of the rod separation (r/r_o), and with more precise expressions of the relationships.

Several other factors which expand still further on the previous study of the effects of the quadrupole collision chamber include the quadrupole length, the axial energy, the diameter of the exit orifice, the radial angle of ion path on the cross section of the quadrupole, the phase of quadrupole radio frequency voltage at the time of ion entry, the ion fragmentation after collision in the chamber, and the time of its fragmentation. Results show that these parameters affect the performance of the RF-only quadrupole. The ratio of the high mass limit to the low mass limit (Mh/Ml) is now also expressed in an equation. Some recommendations to the quadrupole users have been derived from this study.

This chapter is divided into four parts. The introduction provides a brief description of the significance of the study in this chapter, a historical review of computer simulation studies on quadrupole mass filter, and an overview of the present work. The experimental section describes the origin of the computer program, its modification, and its basic principles. The

experimental section also describes the procedure for setting up the quadrupole field for ions, the consequences of choosing parameters for investigations, and the selection of values of parameters for experiments. Following that are detailed results and discussions of the effects of each factor on the low mass limit and on the high mass limit in the RF-only quadrupole chamber. The conclusion section provides a summary of the effects of these factors on quadrupole performance and presents several suggestions and guidelines for quadrupole users on instrumentation, operation, and applications.

Experimental

The computer program which was used in this study was originally developed in J.D.Morrison's laboratory. McGilvery and Morrison used it to calculate ion trajectories, ion distribution, and ion densities in the central quadrupole of their tandem quadrupole mass spectrometer for the study of laser-induced photodissociation of ions [8]. R.A.Yost and C.G.Enke used this program to calculate the ion trajectories in the RF-only central quadrupole of the triple quadrupole mass spectrometer system [4]. This program, which uses digital simulation, was written in Fortran IV. The plotting

subroutine was originally written in Assembly language, but is now changed to Fortran IV. The program has been modified to fit our current PDP 11/40 minicomputer with RSX-11M multiuser operating system [19], 128K words of memory, a cartridge disk, Tektronix graphics terminal, and Printronix graphics printer or Versatec graphics printer. Some functions have been added to allow the selection of graphics terminals, to change the quadrupole length, to perform different types of ion trajectory studies in a single run, and to give adjustable physical dimensions for experimental situations.

The simulation is based the potential equation from quadrupole theory, the equations of ion motion in this quadrupole field, and elementary equations of motion in classical physics. In using this program, the quadrupole electrodes are first built, and then the electric field is developed between them. The voltage, the frequency, the m/z, the position, and the energy of the ion are chosen at the beginning of the experiment. The energy, velocity, and position of an ion are then changed from the original values to succeeding new values according to the fields surrounding the ion. The field produces an acceleration force on the ion of m/z at its initial state. The acceleration is calculated by the equation $F = ma = zE$, where F is the force, m is the mass, a is the acceleration, z is the charge, and E is the electric field. Over a very short time

interval, the acceleration can be considered constant. By using the simple kinetic energy equation $KE = 0.5mv^2$, where KE is the kinetic energy, and v is the velocity, and trigonometric equations, the velocity and position of this ion are then calculated after this small time interval. In succeeding computation cycles, the new acceleration force, velocity, position, and energy are then calculated iteratively.

In selecting the parameters, we started with the actual physical values of the instrument in our laboratory. The quadrupole length is 21.6 cm and the diameter of the central quadrupole rods is 0.954 cm. The ratio of the quadrupole radius to the half length of the separation between opposite electrodes is 1.148 which was reported by Dawson [6] as the optimal value. According to Dawson's study, round rods will produce a field very close to the ideal field which has hyperbolic equipotential lines.

Figure 2-1 shows an equipotential map of the electric field in the quadrupole which has the r/r_o ratio of 1.148. In this map, the difference of electric field between two adjacent lines is constant. After the point-by-point "construction" of the quadrupole electric field as shown, ions are "injected" into this electrostatic field with the electric field changing dynamically with time.

Figure 2-2 shows the radial angle of the ion path entering the quadrupole. This angle θ is expressed in

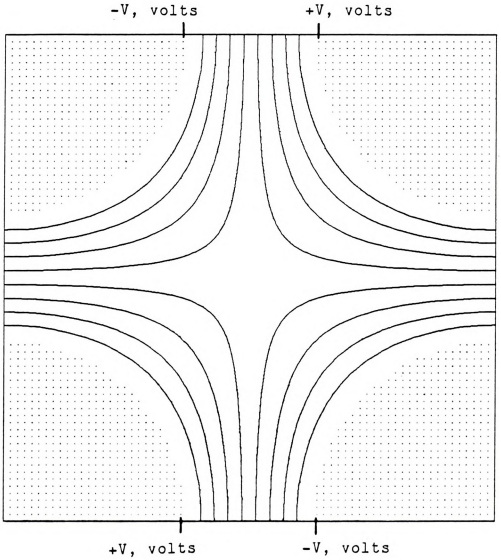

Figure 2-1. An equipotential map of the electric field in the quadrupole. $r/r_o = 1.148$. In this map, the potential difference between two adjacent lines is constant.

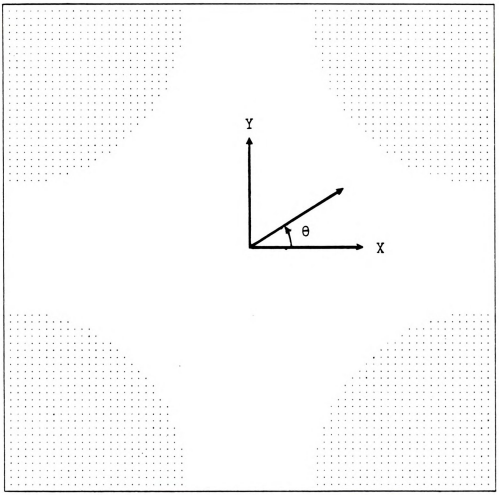

Figure 2-2. The radial angle of the ion path entering the quadrupole. This angle is expressed in degree with respect to x-axis (assuming that z-axis is the axis of the quadrupole).

degrees with respect to the x-axis (assuming that z-axis is the axis of the quadrupole). Figure 2-3 shows the relationship between the radius (r) of the quadrupole rod and the distance (r_o) between the quadrupole rod and the center of the quadrupole.

In the dynamic field, the time resolution of interaction between the ions and the electric field depends on the frequency of the field variation. The time resolution we use is one hundredth of one period of the RF field variation. For example, for a frequency of 1 MHz, the time resolution is one hundredth microsecond. The acceleration considers both the time interval between calculations and the phase of the radio frequency at that time. The mass to charge ratio was chosen to have a value in the range of common interest such as 50, or 100. With these values the program was run to find the ranges of reasonable RF peak voltages at the values of the radio frequency used for our instrument such as 1.0 MHz, 2.4 MHz, 3.0 MHz, and so on. Then the ranges of reasonable frequencies were studied for RF peak voltages of 10, 20, 50, and 100 V, and so on. Ion trajectories were simulated in the quadrupole field with fringing fields ignored. After a number of such trials, the reasonable ranges of the parameters for experiments were obtained.

Having studied the behavior and characteristics of the ion trajectories in the RF-only quadrupole chamber with the

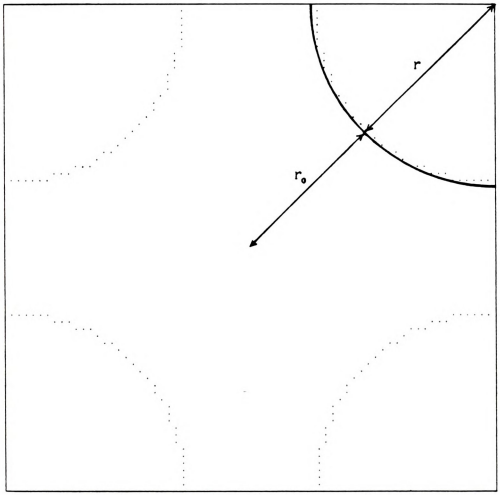

Figure 2-3. The radius (r) of quadrupole rods and the distance (r_o) between the quadrupole rod and the center of the quadrupole.

values of the parameters described above, other parameters were varied one at a time. The ranges of these parameters are as follows: 0.48-3.80 cm diameter rods, 5.4-2160.0 cm electrode length, and the ratio of the quadrupole radius to half the separation between opposite quadrupole electrodes 0.7-1.5. In order to understand the effects of every factor, the simulation studies on the effects of these parameters cover the following ranges: 100 kHz to 40 MHz, 10-4000 V peak RF, 0-3.5 eV of ion off-axis energy, 5-80 eV axial energy, exit orifice diameters of 0.5-4.0 mm, radial angles of ion entry from 0-360 degrees with 5 or 10 degree increments, the phase of quadrupole radio frequency at the time of ion entry from 0-360 degrees with 5 or 10 degree increments, the mass of the daughter ions in fragmentation process from 33-36 m/z, fragmentation time of 1.25-20.00 us, and ions of mass to charge ratio from 1 to 1,000,000.

The trajectory routes and patterns depend on the specific combinations of the parameters. The ion's direction of motion, its position, and its velocity are constantly changing. Whenever the change of the direction of motion is smaller, the velocity of the ion becomes greater. After several cycles, the outer boundaries of many of the stable ion trajectories form regular shapes such as ellipses, circles, lines, rectangles, parallelograms, or squares.

Figure 2-4 shows an example of an ion trajectory in the RF-only quadrupole chamber of the triple quadrupole mass spectrometer for the combination of parameters given. The ion moves around the center of the quadrupole in a somewhat symmetrical route. After traveling 30 microseconds, the outer boundary of this ion trajectory is somewhat rectangular.

Figure 2-5 shows relationships between ion's traveling time in the quadrupole and the radial angle, the distance to the center, and ion's off-axis energy, for the example of ion trajectory shown in Figure 2-4. The ion's radial angle, its distance, and its energy are changing constantly. Their relationship is not completely obvious.

The low mass limits and the high mass limits were determined by running the computer simulation program to examine the stability of the ion's trajectory. The determination of the mass limit was made by trial and error. For example, in finding the low mass limit, a low mass value was input into the program to examine whether this ion was stable (would pass the the quadrupole). If this ion was stable, a smaller value would be chosen for the next run. If it was unstable, a larger value would be chosen. The lowest possible mass to charge ratio that was stable was the low mass limit. In finding the high mass limit, a large mass value was input to examine whether this ion was stable. If so, a larger value would be chosen for the next run.

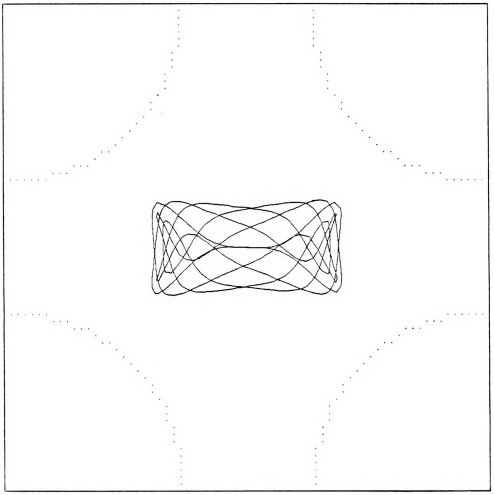

Figure 2-4. The computer simulated ion trajectory of an ion in the RF-only quadrupole of TQMS. RF peak voltage = 20 V, Frequency = 0.6 MHz. r/r_o = 1.148. Diameter of Rods = 1.9 cm. Mass = 40 (M/z). Off-axis energy = 0.8 eV. Radial angle of the ion entering the quadrupole = 0 degree. Initial phase = 0 degree. Time = 30 μs.

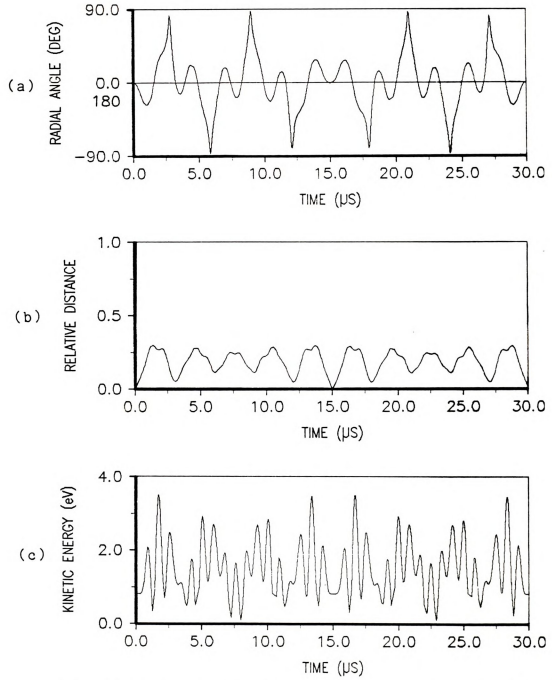

Figure 2-5. Relationships between ion's traveling time (μs) in the RF-only quadrupole of TQMS and (a) the radial angle (with respect to x-axis, in deg.) (b) the distance to the center of quadrupole (compared with the distance between the center of the quadrupole and the center of rods) (c) the off-axis energy (eV), for the ion trajectory shown in Figure 2-4. Parameters are the same as those in Figure 2-4.

Otherwise, a smaller value would be chosen. The highest possible stable mass to charge ratio was the high mass limit.

Preliminary trials provided the reasonable ranges for the values of most experimental parameters. Unless the parameter chosen is the variable, the values of the parameters used in this chapter have the following values: the diameter of the quadrupole electrode rods is 0.954 cm. the rod length is 21.6 cm, the ratio of the quadrupole radius to the half length of the separation between opposite quadrupole electrodes is 1.148, the radio frequency is 600 KHz, the peak voltage is 20.0 V, the radial angle of the ion path entering the quadrupole is 0 degree, the initial phase of quadrupole radio frequency is 0 degree, the ion's off-axis energy is 1.0 eV, and the axial energy is 20.0 eV.

Results and Discussion

Many parameters affect the characteristics of ion trajectories in the RF-only quadrupole chamber in TQMS. Their effects have been studied by varying only one parameter at a time. The values of the parameters follow the constant values given in the last part of previous section, except the parameter which is under investigation and is changed as indicated in tables or in figures.

Effects of RF Voltage and Frequency

Table 2-1 shows the effects of the RF voltage and frequency on the mass limits of ion transmission through the quadrupole. This table demonstrates a trend exists in the case of each relationship, between the low mass limit and the voltage, between the low mass limit and the frequency, between the high mass limit and the voltage, and between the high mass limit and the frequency. When the radio frequency is held at 2.4 MHz and the peak voltage changes from 10 to 500 volts, the low mass limit is proportional to the voltage applied on the quadrupole rods, and the high mass limit is proportional to the voltage squared. For another group of experiments, the radio frequency is set at 600 kHz and the voltage varied from 5 to 500 volts and the same relationship between the peak voltage and both mass limits is observed. Looking at the case of constant peak voltage while varying only the frequency, we get another relationship between the frequency and the mass limits. At 100 V, the frequency was given values from 0.3 to 4.8 MHz, both the low mass limit and the high mass limit are inversely proportional to the frequency squared. The same trends are observed when the peak voltage is 10 V and the frequency varies from 100 kHz to 2.4 MHz.

Figure 2-6 shows the relationships, by log values, between both mass limits and the radio frequency at the

Table 2-1. Effects of RF frequency and peak voltage on mass limits*

F (MHz)	2.4	2.4	2.4	2.4	2.4
V (volt)	10	20	50	100	500
Ml (M/z)	1.15	2.04	4.79	9.45	46.7
Mh (M/z)	2.97	12.0	75.3	301	7.52×10^3

F (MHz)	0.6	0.6	0.6	0.6	0.6	0.6
V (volt)	5	10	20	50	100	500
Ml (M/z)	-	17.2	32.5	76.6	151	746
Mh (M/z)	-	47.5	192	1.20×10^3	4.82×10^3	1.20×10^5

F (MHz)	0.3	0.6	1.2	2.4	4.8
V (volt)	100	100	100	100	100
Ml (M/z)	605	151	37.8	9.45	2.37
Mh (M/z)	1.92×10^4	4.82×10^3	1.20×10^3	301	75.3

F (MHz)	0.3	0.6	1.2	2.4
V (volt)	10	10	10	10
Ml (M/z)	68.6	17.2	4.60	1.15
Mh (M/z)	190	47.5	11.8	2.97

* F = RF frequency (MHz). V = RF peak voltage (V). Ml = Low mass limit (M/z). Mh = High mass limit (M/z). Diameter of electrode rods = 9.54 mm. Off-axis eneergy = 1.0 eV. Axial energy = 20.0 eV.

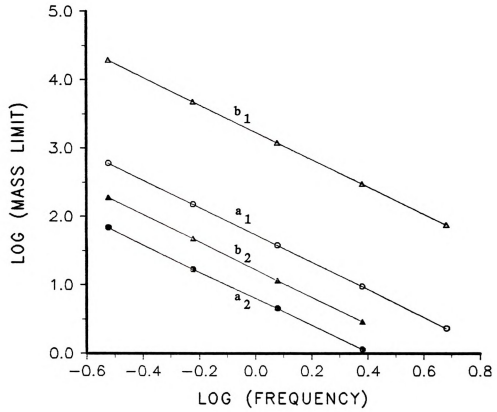

Figure 2-6. Relationships between the RF frequency and mass limits. (a1) log(M1) vs. log(F) at voltage = 100 V. (a2) log(M1) vs. log(F) at voltage = 10 V. (b1) log(Mh) vs. log(F) at voltage = 100 V. (b2) log(Mh) vs. log(F) at voltage = 10 V. F = RF frequency (MHz). V = peak voltage(V). M1 = Low mass limit (M/z). Mh = High mass limit (M/z).

conditions of 10 and 100 V. This plot gives straight lines between log(Ml) vs. log(F), or log(Mh) vs. log(F). All the slopes of these lines have the value of -2. This indicates that both the low mass limit and the high mass limit are inversely proportional to the frequency squared.

Figure 2-7 shows the relationships between the peak voltage and both mass limits. On this plot, Lines a1 and a2 give the relationships between the low mass limit and the peak voltage for the frequencies 2.4 MHz and 0.6 MHz, respectively. They both have a slope of 1. This indicates that the low mass limit is directly proportional to the peak voltage. Lines b1 and b2 show the relationships between the high mass limit and the peak voltage for the frequencies 2.4 MHz and 0.6 MHz, respectively. They both have a slope of 2. This indicates that the high mass limit is proportional to the voltage squared. Two equations are empirically obtained for the relationship between both mass limits and the voltage and the frequency.

$$M_l = \frac{0.533\ V}{F^2} + 2.9 \qquad \text{----- (2-1)}$$

$$M_h = \frac{0.173\ V^2}{F^2} \qquad \text{----- (2-2)}$$

where Ml is the low mass limit in the mass to charge ratio, Mh is the high mass limit in the mass to charge ratio, V is the peak voltage (volt), F is the RF frequency (MHz).

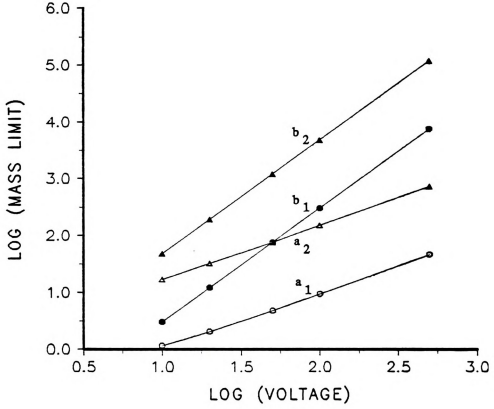

Figure 2-7. Relationships between the RF peak voltage and mass limits. (a1) log(Ml) vs. log(V) at F = 2.4 MHz. (a2) log(Ml) vs. log(V) at F = 0.6 MHz. (b1) log(Mh) vs. log(V) at F = 2.4 MHz. (b2) log(Mh) vs. log (V) at F = 0.6 MHz. F = RF frequency (MHz). V = peak voltage (V). Ml = Low mass limit (M/z). Mh = High mass limit (M/z).

Table 2-2. Effects of off-axis energy on mass limits*

Eoa (eV)	0	0.01	0.05	0.10	0.25	0.50
Ml (M/z)	24.7	29.7	29.9	30.0	30.4	31.0
Mh (M/z)	$>10^6$	$>10^6$	4.09×10^3	1.93×10^3	770	385

Eoa (eV)	1.00	1.50	2.00	2.50	3.00	3.50
Ml (M/z)	32.5	34.2	37.2	42.6	55.1	-
Mh (M/z)	192	127	95.0	75.4	62.5	-

* Eoa = off-axis energy (eV)

Effect of Ion's Off-axis Energy

The effect of the ion's off-axis energy on the mass limits is shown in Table 2-2. The value of the ion's off-axis energy is varied, but the other parameters have the same values as given in the last paragraph of the experimental section. When the ion's off-axis energy increases from 0.05 to 3.00 eV, the high mass limit is inversely proportional to this energy except at the extreme case of zero or very low off-axis energy. The off-axis energy has a very small affect on the low mass limit except in the case of relatively large or zero off-axis energy. Ions with off-axis energy greater than 3.50 eV will not pass the quadrupole. Figure 2-8 shows the relationship between

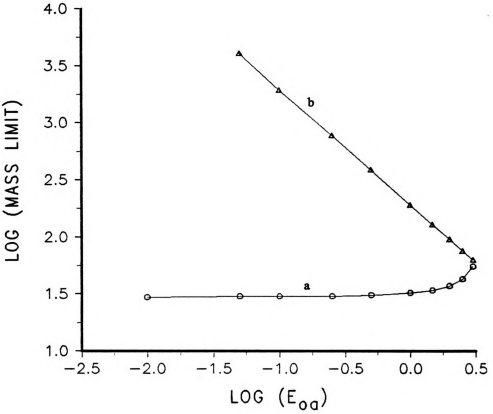

Figure 2-8. Relationships between the off-axis energy and mass limits. (a) log(Ml) vs. log(Eoa). (b) log(Mh) vs. log(Eoa). Eoa = Off-axis energy (eV). Ml = Low mass limit (M/z). Mh = High mass limit (M/z).

the off-axis energy and both mass limits. The left four-fifths of line a is nearly straight and constant in value. This indicates that the low mass limit is nearly independent of the ion's off-axis energy, except for very low or high energy. The two lines intersect at the value below 3.50 eV off-axis energy. These results imply that the smaller the divergence of the ion path, the better the transmission.

This study also shows that the off-axis energy has a greater effect on the high mass limit and will cut the transmission of ions with high mass to charge ratio. It is desirable to reduce the off-axis energy of ions by directing the ion paths to be parallel to the longitudinal axis of the quadrupole, focusing the ions close to the center of the cross section of the quadrupole. This can be achieved by improving the design of the ion source and the setting and operation of the lens system.

Effect of Quadrupole Cross Section

Data in Table 2-3 reveal the dependence of mass limits on the quadrupole cross section with constant ratio of the quadrupole radius to the half length of the separation between opposite quadrupole electrodes. These data are plotted in Figure 2-9. Line a or Line b, or the equivalent, log(Ml) vs. log(D) or log(Mh) vs. log(D), shows the

Table 2-3. Effects of quadrupole cross section on mass limits*

D (mm)	4.77	9.54	19.1	38.2
Ml (M/z)	133	32.5	8.06	2.02
Mh (M/z)	768	192	48.0	12.3

* D = Diameter of electrode rods (mm)

relationship between the quadrupole cross section and the low mass limit or the high mass limit, respectively. Both lines have a slope of -2. This indicates that both the low mass limit and the high mass limit are inversely proportional to the quadrupole cross section or the square of quadrupole diameter. These data imply that the mass range increases as the quadrupole cross section decreases at the condition of constant ratio of the quadrupole radius to the half length of the separation between opposite electrodes.

Depending on the needed range in mass limits, one must select the optimal value for the diameter of electrode rods for the instrument. In addition, one needs also to consider the space between quadrupole rods. When one wants to increase both mass limits by reducing the diameter of electrodes, the space between rods for collision, fragmention, and scattering will also be reduced. Therefore, it is better to provide enough space and adjust

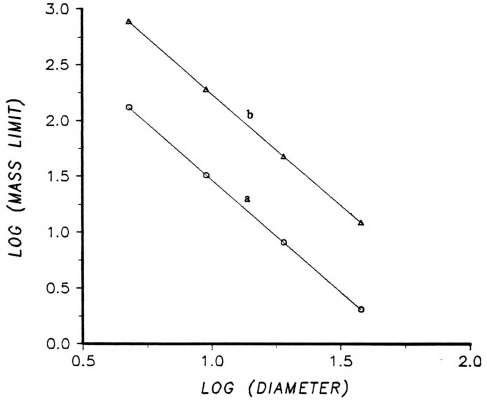

Figure 2-9. Relationships between the quadrupole cross section and mass limits. (a) log(Ml) vs. log(D). (b) log(Mh) vs. log(D). D = Diameter of electrode rods (mm). Ml = Low mass limit (M/z). Mh = High mass limit (M/z).

the frequency or the voltage for passing ions of higher or lower mass to charge ratio. With other parameters constant, simple equations express the relationship observed among both mass limits and the parameters varied in previous tables and figures:

$$M_l = \frac{0.488\ V}{F^2 d^2} + 2.28 \quad \text{----- (2-3)}$$

$$M_h = \frac{0.158\ V^2}{F^2 d^2 E} \quad \text{----- (2-4)}$$

where d is the diameter of the quadrupole rods (cm), E is the off-axis energy (eV).

Effect of r/r_o Ratio

Table 2-4 lists the effects on both mass limits by the ratio of the quadrupole radius to the half length of the separation of quadrupole electrodes for nine different ratios in three sets of voltage and frequency combinations. Figure 2-10 shows the relationship between the r/r_o ratio and both mass limits. Lines a1, b1, and c1 give the plots of log(M1) vs. $\log(r/r_o)$ at the conditions of the peak voltages and frequencies, 20 V and 0.6 MHz, 20 V and 2.4 MHz, and 100 V and 2.4 MHz, respectively. They all have nearly unity slope. This indicates that the low mass limit is directly proportional to the r/r_o ratio. Lines a2, b2,

Table 2-4. Effects of the r/r_o ratio on mass limits*

r/r_o		0.7	0.8	0.9	1.0	1.148	1.2	1.287	1.4	1.5
a	M1	21.8	24.7	27.3	29.8	32.5	34.6	36.8	40.2	44.8
	Mh	39.4	80.0	102	127	192	227	248	324	433
b	M1	1.36	1.45	1.60	1.76	2.02	2.16	2.30	2.52	2.80
	Mh	3.71	5.00	6.43	7.98	12.0	14.2	15.5	20.2	27.0
c	M1	5.96	6.54	7.27	8.16	9.45	9.77	10.8	11.8	12.7
	Mh	94.9	126	126	200	301	354	390	506	575

* r = Radius of quadrupole rods (mm). r_o = Half length of the separation between opposite electrode rods (mm). M1 = Low mass limit (M/z). Mh = High mass limit (M/z). a: Voltage = 20 V, Frequency = 0.6 MHz. b: Voltage = 20 V, Frequency = 2.4 MHz. c: Voltage = 100 V. Frequency = 2.4 MHz.

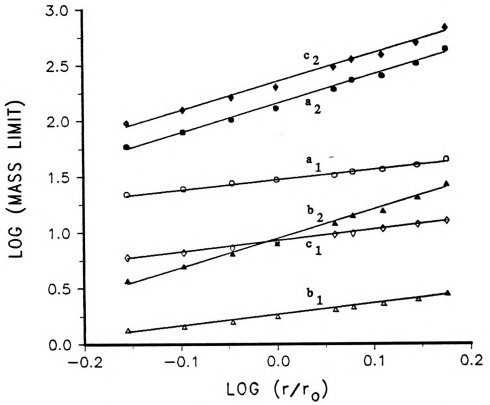

Figure 2-10. Relationships between the r/r_o ratio and mass limits. (a1) log(Ml) vs. $\log(r/r_o)$ at frequency = 0.6 MHz, voltage = 20 V. (a2) log(Mh) vs. $\log(r/r_o)$ at frequency = 0.6 MHz, voltage = 20 V. (b1) log(Ml) vs. $\log (r/r_o)$ at frequency = 2.4 MHz, voltage = 20 V. (b2) log(Mh) vs. $\log (r/r_o)$ at frequency = 2.4 MHz, voltage = 20 V. (c1) log(Ml) vs. $\log(r/r_o)$ at frequency = 2.4 MHz, voltage= 100 V. (c2) log(Mh) vs. $\log (r/r_o)$ at frequency = 2.4 MHz, voltage = 100 V.

and c2 give the plots of log(Mh) vs. $\log(r/r_0)$ at conditions of the peak voltages and frequencies, 20 V and 0.6 MHz, 20 V and 2.4 MHz, and 100 V and 2.4 MHz, respectively. They have nearly the same slope of 2.5. This indicates that the high mass limit is proportional to the five halves power of the r/r_0 ratio.

These results demonstrate again the significant effects on both mass limits, not only by the voltage and the frequency, but also by the ratio of the radius to the half length of the separation of quadrupole. The low mass limit has a commensurable relationship to the ratio value. The high mass limit is approximately proportional to $(r/r_0)^{2/5}$. Either from the data in Table 2-4 or from the plot in Figure 2-10, we can see that the mass range increases as the r/r_0 ratio increases. For example, under the condition of the peak voltage 20 V and the frequency 0.6 MHz, the mass ranges are about 38 and 389 m/z at the r/r_0 ratio of 0.7 and 1.5, respectively. The increase in the mass range is about ten fold. The traditional r/r_0 ratio of 1.148 has a mass range of about 160 m/z. These comparisons show that the higher the r/r_0 ratio, the wider the mass range, due largely to the increase in high mass ions. This suggests that increasing the r/r_0 ratio, with enough distance between adjacent electrodes to avoid spark and consequent electric shutdown, will provide a better RF-only quadrupole chamber with a better transmission of ions and a larger mass range. The

two equations described above can be expressed as follows:

$$M_l = \frac{0.42\ V}{F^2 d^2} \left(\frac{r}{r_o}\right) + 2.30 \qquad \text{----- (2-5)}$$

$$M_h = \frac{V^2}{9F^2 d^2 E} \left(\frac{r}{r_o}\right)^{5/2} \qquad \text{----- (2-6)}$$

The relationship between the high mass limit and the low mass limit can be expressed in Equation 7 at the conditions with the same values for the RF voltage, the frequency, the cross section of quadrupole rods, the r/r_o ratio, and the length for the rods.

$$\frac{M_h}{M_l} = \frac{0.263\ V}{E} \left(\frac{r}{r_o}\right)^{3/2} - 0.50 \qquad \text{----- (2-7)}$$

This equation demonstrates a significant possibility for increasing the ratio of the high mass limit to the low mass limit, and hence the mass range. This ratio can be increased by increasing the voltage or the r/r_o ratio, or by decreasing the off-axis energy.

Equations 5, 6, and 7 provide a guide in choosing the parameters for new instrumentation, operation of the instrument, and the accessible range of applications. After choosing the combination of the electrode rod cross section, the r/r_o ratio, and the length for the rods, the combination of the peak voltage and the radio frequency can be chosen for the desired mass range.

Effect of Quadrupole Length

The length of the quadrupole has a very small effect on either mass limits. Table 2-5 indicates that the high and low mass limits are almost constant when the quadrupole length is increased stepwise from 10.8 to 2160.0 cm with an exception at the very short length. The quadrupole length of 21.6 cm, the dimension of our central quadrupole, is adequate from the standpoint of passing the ions in the range of interest. There are several factors in considering the optimal length for the quadrupole: the chamber needs enough length for collision purpose at a certain pressure of the reagent gas, the quadrupole needs enough length for the focusing effect to achieve its role, the screen effect of the quadrupole prefers short length so this effect does not reduce too much transmission, and a compact instrument desires a shorter length. A shorter quadrupole such as that of 10.8 cm may be used if the pressure of the reagent gas is high enough for collision.

Effect of Ion's Axial Energy

Table 2-6 shows the effects of the ion's axial energy on both high and low mass limits. These results point out that the axial energy has nearly no effect on the low and high mass limits without exit orifice (Ml, Mh), and has very

Table 2-5. Effect of quadrupole length on mass limits*

QL	2.7	5.4	10.8	21.6	43.2	86.4	216	2160
Ml	24.7	32.3	32.3	32.5	33.1	33.9	34.3	34.3
Mh	$>10^6$	196	192	192	192	192	192	192

* QL = Length of quadrupole rods (cm)

Table 2-6. Effect of axial energy on mass limits*

Eax	5	10	15	20	30	40	50	60	70	80
Ml	34	33	33	33	33	33	33	33	33	33
Mlo	35	33	33	35	33	34	35	33	37	34
Mho	192	186	190	188	177	192	191	191	190	189
Mh	192	192	192	192	192	192	192	192	192	192

* Eax = Axial energy (eV).
  Ml = Low mass limit without exit orifice.
  Mlo = Low mass limit with exit orifice.
  Mho = High mass limit with exit orifice.
  Mh = High mass limit without exit orifice.

Table 2-7. Effect of diameter of exit orifice on mass limits*

Reo	0.25	0.50	1.00	1.50	2.00
Ml	33	33	33	33	33
Mlo	66	50	40	40	35
Mho	146	147	187	187	188
Mh	192	192	192	192	192

* Reo = Radius of exit orifice (mm).
  Ml = Low mass limit without exit orifice.
  Mlo = Low mass limit with exit orifice.
  Mho = High mass limit with exit orifice.
  Mh = High mass limit without exit orifice.

small, irregular effect on the low and high mass limits with exit orifice (Mlo, Mho). This suggests that the axial energy is not an important factor in the consideration for the transmission of ions. Therefore, if the voltage of the repeller is scanned along the experiment, the mass limits will not be much affected.

Effect of Diameter of Exit Orifice

Table 2-7 shows that the diameter of the exit orifice doesn't affect Ml and Mh, but does affect Mlo and Mho. When the diameter of the exit orifice increases, Mlo decreases, Mho increases, and thus the mass range of passing ions

increases. This reveals that in order to increase the transmission, considering only the factor of the exit orifice diameter, one should increase the diameter of the exit orifice. This will pass a larger mass range of ions.

Effect of Radial Angle

The radial angle of the ion path entering the quadrupole, along the longitudinal axis and imaging the radial angle on the plane perpendicular to the longitudinal axis, has some effects on the mass limits and is shown on Table 2-8. The effect on all mass limits by the radial angle between 0 and 180 degrees is the same as that between 180 and 360 degrees. The radial angle has a very small effect on both low mass limits (Ml, Mlo), but has a large, uneven effect on both high mass limits (Mh, Mho).

Effect of Phase of RF Frequency

The effect on mass limits by the phase of the quadrupole radio frequency at the time of ion entry is shown in Table 2-9. The phase almost doesn't change either high mass limits (Mh, Mho), but has a small effect on both low mass limits (Ml, Mlo). This effect repeats every 180 degrees.

Table 2-8. Effect of angle of the ion path entering the quadrupole on mass limits*

θ	0	10	20	30	40	45	50	60	70	80
Ml	33	35	35	35	38	37	38	35	35	35
Mlo	35	35	39	35	38	37	38	35	39	35
Mho	188	203	113	103	109	75	109	103	113	203
Mh	192	204	235	110	118	107	118	110	235	205

θ	90	100	110	120	130	135	140	150	160	170
Ml	33	33	33	35	38	38	38	35	33	33
Mlo	35	34	34	39	40	40	40	39	34	34
Mho	187	205	114	105	76	78	76	105	114	205
Mh	192	207	160	120	103	104	103	120	161	207

θ	180	190	200	210	220	225	230	240	250	260
Ml	33	35	35	35	38	37	38	35	35	35
Mlo	35	35	39	35	38	37	38	35	39	35
Mho	188	203	113	103	109	75	109	103	113	203
Mh	192	204	235	110	118	107	118	110	235	205

θ	270	280	290	300	310	315	320	330	340	350
Ml	33	33	33	35	38	38	38	35	33	33
Mlo	35	34	34	39	40	40	40	39	34	34
Mho	187	205	114	105	76	78	76	105	114	205
Mh	192	207	160	120	103	104	103	120	161	207

θ = Angle of the ion path entering the quadrupole (deg.).

Table 2-9. Effect on mass limits by initial phase of quadrupole radio frequency at the time of ion entry*

P	0	10	20	30	40	45	50	60	70	80
Ml	33	34	35	35	37	37	37	34	39	39
Mlo	35	35	35	40	40	40	40	40	39	39
Mho	188	188	188	188	189	188	188	188	188	189
Mh	192	192	192	192	192	192	192	192	192	192

P	90	100	110	120	130	135	140	150	160	170
Ml	39	39	38	37	36	35	35	31	34	33
Mlo	39	39	39	40	40	35	36	31	34	34
Mho	189	188	188	188	188	188	188	188	188	188
Mh	192	192	192	192	192	192	192	192	192	192

P	180	190	200	210	220	225	230	240	250	260
Ml	33	34	35	35	37	37	37	34	39	39
Mlo	35	35	35	40	40	40	40	40	39	39
Mho	188	188	188	188	187	188	188	188	188	189
Mh	192	192	192	192	192	192	192	192	192	192

P	270	280	290	300	310	315	320	330	340	350
Ml	39	39	38	37	36	35	35	31	34	33
Mlo	39	39	39	40	40	35	36	31	34	34
Mho	189	188	188	188	188	188	188	188	188	188
Mh	192	192	192	192	192	192	192	192	192	192

* P = Initial phase (deg.) of quadrupole radio frequency at the time of ion entry.

Table 2-10. Effect of fragmentation on mass limits*

θ	0	0	0	0	20	20	20	20
Mf	33	34	35	36	33	34	35	36
Ml	33	34	33	36	39	35	35	36
Mlo	59	35	35	58	42	35	37	37
Mho	111	118	112	119	121	121	125	121
Mh	116	118	117	119	123	125	125	126

* θ = Angle of ion path entering the quadrupole (deg.).
Time of dissociation = 10 μ sec.
Mf = Mass of fragment ion (M/z).

Effects of Fragmentation and Fragmentation Time

Table 2-10 shows the effect on the four mass limits by the fragmentation after collision in the chamber. The mass limits of the parent ions were studied with different daughter ions having a mass-to-charge ratio between 33 and 36 and entering the quadrupole with radial angle of 0 and 20 degrees. In both cases at different radial angles, the fragmentation effect is complex. The effect of the ion's fragmentation time on the mass limits of parent ions is also complex, as shown in Table 2-11.

Table 2-11. Effect of fragmentation time on mass limits*

Mf	33	33	33	33	33	33	34	34	34	34	34	34
Td	1.25	2.5	5.0	10.0	15.0	20.0	1.25	2.5	5.0	10.0	15.0	20.0
Ml	33	33	33	33	33	33	34	34	34	34	34	34
Mlo	79	36	-	59	35	35	40	35	35	35	35	35
Mho	>79	41	-	111	156	112	>40	44	66	118	155	114
Mh	>78	43	63	116	158	113	>34	44	66	118	159	114

Mf	35	35	35	35	35	35	36	36	36	36	36	36
Td	1.25	2.5	5.0	10.0	15.0	20.0	1.25	2.5	5.0	10.0	15.0	20.0
Ml	35	35	35	35	35	35	36	36	36	36	36	36
Mlo	35	35	35	35	35	35	37	37	37	58	45	40
Mho	>35	41	66	112	89	111	>37	41	65	116	155	181
Mh	>35	46	67	117	89	114	>36	48	67	119	160	181

* Mf = Mass of fragment ion (M/z).
  Td = Time of dissociation (μ sec.)

Conclusions

The many variables studied in this paper affect the low mass limit and the high mass limit of the transmission of ions through the RF-only quadrupole. The low mass limit is directly proportional to the peak voltage and the r/r_o ratio, but inversely proportional to the frequency squared and the electrode cross section. It is not much affected by the quadrupole length, the ion's off-axis energy, its axial energy, the radial angle of the ion path entering the quadrupole, the initial phase of the frequency at the time of ion entry, the ion's fragmentation, or its fragmentation time. The high mass limit is proportional to the peak voltage squared, and to the five halves power of the r/r_o ratio, but inversely proportional to the frequency squared, the electrode cross section, and the off-axis energy. It is not much affected either by the quadrupole length except for very short lengths, or by the axial energy, the initial phase of the quadrupole radio frequency, or the ion's fragmentation. The diameter of the exit orifice has uneven effects on both the high and low mass limits for passing the ions through the quadrupole. The radial angle of the ion path on the cross section of the quadrupole, the ion's fragmentation, and the time of its fragmentation have uneven effects on high mass limits(Mh, Mho). Therefore, these parameters play more or less important roles in the

performance of the TQMS.

Some recommendations are derived from this study for the users for maximizing the ratio of the high mass limit to the low mass limit (Mh/Ml). Equation 7 shows that the Mh/Ml ratio is proportional to the RF voltage, proportional to the three halves power of the r/r_o ratio, and inversely proportional to the off-axis energy. For the normal application of the quadrupole, an increase in the RF voltage will increase the Mh/Ml ratio proportionally. By applying appropriate voltages on the lens system to decrease the ion's off-axis energy, the transmission and thus the sensitivity of ions of high mass to charge ratio will increase. For those who construct a non-standard central quadrupole, an increase on the r/r_o ratio will increase the Mh/Ml ratio by the three halves power of the r/r_o ratio. For example, a change in the r/r_o ratio from the regular value of 1.148 to 1.5, will increase the Mh/Ml ratio up to two and a half fold. Keeping enough distance between adjacent electrodes to avoid spark and consequent electric shutdown, an increase in the r/r_o ratio will provide a better RF-only quadrupole chamber with a better transmission of ions, especially for ions of high mass to charge ratio.

Besides the above recommendations, several guidelines for instrumentation, operation, and applications of quadrupole devices are suggested by this study. In analytical instrumentation, if one wants to detect ions of

very high mass to charge ratio, a quadrupole with a smaller cross section for electrode rods can be constructed because both mass limits are inversely proportional to the cross section. In order to increase the transmission, the diameter of the exit orifice can be increased. In the operation of quadrupole devices, if one wants to detect ions of higher mass to charge ratio, a higher RF voltage or a lower frequency should be chosen. The reasons are that the low mass limit is proportional to the voltage and inversely proportional to the frequency squared, and that the high mass limit is proportional to the voltage squared and inversely proportional to the frequency squared. To find the accessible mass range for analytical and theoretical applications, reasonable combinations of the RF peak voltage and the frequency for new experiment can be derived from known combinations of the voltage and the frequency used in previous experiments.

CHAPTER 3

COMPUTER-AIDED ION SOURCE DESIGN : EFFECTS OF REPELLER ELECTRODE SHAPE

Introduction

Since Nier developed his ion source in 1940 and modified it in 1947, most electron impact ion sources in modern analytical mass spectrometers are based on his design. Because the ion source efficiency is the limiting factor in many types of mass spectrometers, it is important to study means for its improvement. To this end, many variations in the ion source designs have been reported.

Fock [20] designed a mass spectrometer based on computed ion trajectories in 1969. He presented an ion source of the Nier type by adding a "repeller" field. In that paper he showed how the presence of the "repeller" field can reduce the asymmetry of a set of trajectories and improve the imaging property of the source. Beg and Malik [21] used the high power density electron impact technique to develop a metal ion source. Coforti et al.[22] designed an alkali ion source by the aid of computer calculation. The source geometry and electrode potentials were optimized by simulation of ion trajectories. The focusing system employed consists of a Pierce extractor and a lens.

Recently, Koontz and Denton [23] described a very high yield EI source for the determination of organic compounds. This Penning source produces higher useful ion currents and better signal-to-noise ratios than conventional Nier type sources.

Many CI mass spectrometers are operated by using a Nier type EI source with some modifications. These include the diminution of the size of the ion exit slit and electron entrance aperture, to prevent electrical breakdowns, to get a gas tight connection between the inlet system and the source, and to maintain pressure differential ratio of about 10 between source chamber and source housing.

Michnowicz and Munson [24] made some modifications to allow the operation of a CEC-21-1108 mass spectrometer source at pressure of 0.5 torr. Beggs and Vestal [25] designed and constructed a CI source for operation at ion chamber pressures up to 2 torr. An interesting feature in their design is that the repeller is in a concave, half-cylindrical shape, with the gas and sample entering through a hole in the ion repeller. This source is capable of both EI and CI modes. Chang, Sroka and Meisels [26] studied the effects of geometry of CI ion source on mean residence times in the source and arrival time distributions. Hoegger and Bommer [27] designed and constructed a CI ion source which uses low energy ions produced in a high frequency flow discharge.

Hunt et al.[28] reported a CI source utilizing a Townsend discharge to ionize the reagent gas. This source generated both positive and negative CI spectra with a wide variety of either oxidizing or reducing reagent gases. Kambara and Kanomata [29] employed a needle electron source. A survey of instrument technology on CI mass spectrometry was presented by Mather and Todd [30]. Hogg and Payzant [31] designed a combined field ionization/field desorption/electron impact (FI/FD/EI) ion source. It was stated that switching between the FI/FD and EI modes is simple and fast.

A lot of effort to increase the efficiency of ion sources has been made as described in the previous studies. The ion source designs presented in this chapter offer further improvement in source efficiency and demonstrate the value of computer modeling in ion source design.

Experimental

In this work, several different ion source designs by computer simulation of the ion trajectories were studied. The first study was the ion source which was used with our mass spectrometer as shown in Figure 3-1. The computer set up the components of the ion source and calculated the electric field in it. Ions were placed at different

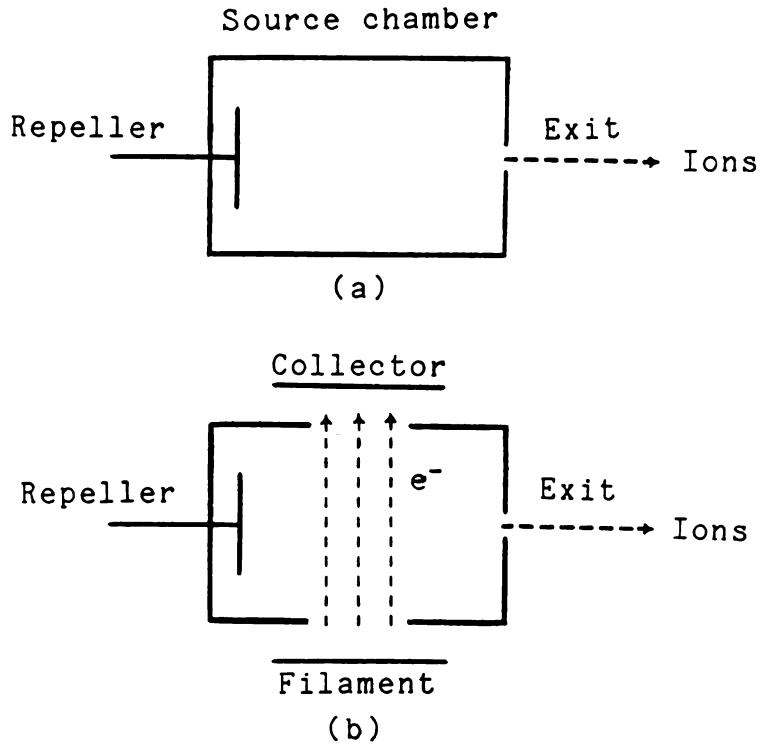

Figure 3-1. Schematic diagram of the ion source used in our triple quadrupole mass spectrometer, (a) top view, and (b) side view.

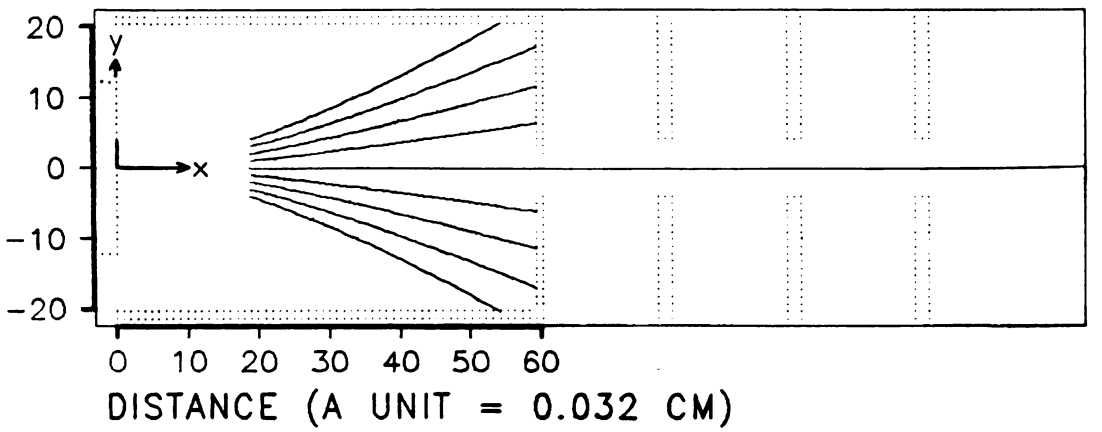

Figure 3-2. Some trajectories of ions formed in the ionization chamber of the EI source used in our mass spectrometer.

positions in the ion source with zero initial kinetic energy. The computer calculated the acceleration force on ions due to the electric field at their location. Under this acceleration force ions began to move and their trajectories were then calculated. The ions' final positions, energies, directions of motion, and time of flight were printed on the terminal. Ion trajectories and the equipotential map inside this source were studied by plotting them on the CRT. From the results of ion trajectory calculations, the performance of the source was determined.

After gaining some understanding of the bases for some of the characteristics of this source, some possibilites for improvement came to mind. Then new ion source designs were tested by computer program to observe the effects of new shapes and/or different potentials. The components in a new ion source were "built" by specification to the computer, and the electric field in the source was developed. In the same way, ions were placed inside the new source one by one with zero initial kinetic energy. The acceleration forces, ion trajectories, final positions, energies, directions of motion, and times of flight for ions in the new source were calculated. Ion trajectories and the equipotential map for each source were plotted to study the characteristics of each source. The performance of each source was determined amd was compared with that of the original source. These

comparisons suggest guidelines for selecting ion source designs for real construction.

These studies also showed that the ion trajectories inside the ion source are the same for ions of different mass to charge ratios. From the studies of equipotential maps and the outcome of ions' kinetic energies, a new ion source for producing an abundance of ions with small kinetic energy spread was designed. For this source, the equipotential map, ion trajectories, performance, ion residence time, and the ion kinetic energy at the chamber exit were examined.

Results and Discussions

Volumes of Stable Trajectories

Figure 3-2 shows a scale drawing of the EI source first used on our mass spectrometer and shows the trajectories of ions formed in this source. This figure reveals that most ions form divergent trajectories with respect to the center of the repeller or the ion source exit. The figure demonstrates that only a small fraction of the ions formed in this source design will pass the exit. The ion trajectories inside the ion source are found to be independent of mass to charge ratio.

In Figure 3-2, the voltages of the repeller and of the chamber are 40 V and 10 V, respectively. The front center of the repeller is assigned x and y spatial coordinate values of 0. The x value at the center of ion source exit is 60, and the y value at the inner top of ionization chamber is 20, with each unit of length equal to 0.032 cm. The electron entrance is a slot with x values from distance units 18 to 42 at a y value of -20.

As shown in Figure 3-3, the reason for the poor efficiency of this ion source in producing focused ion current is the inverted bowl-shaped electric field as shown by the equipotential "contour" lines. The ions formed in the ionization chamber suffer defocusing force for a wide range, long distance, and all space; only those formed almost exactly on the line between the centers of the repeller and the exit slit can emerge.

Following this same procedure, the characteristics of several new ion source designs have been studied. In these designs, only the shapes inside the ionization chamber are varied, keeping the condition of the outside lenses the same. It was found that by just changing the shape of the repeller, the size of the volume in which ions formed will pass the exit of the chamber can be increased to a large extent. It is assumed that this will cause a corresponding improvement in ionization efficiency. The better designs are those in which the chamber is divided into two main

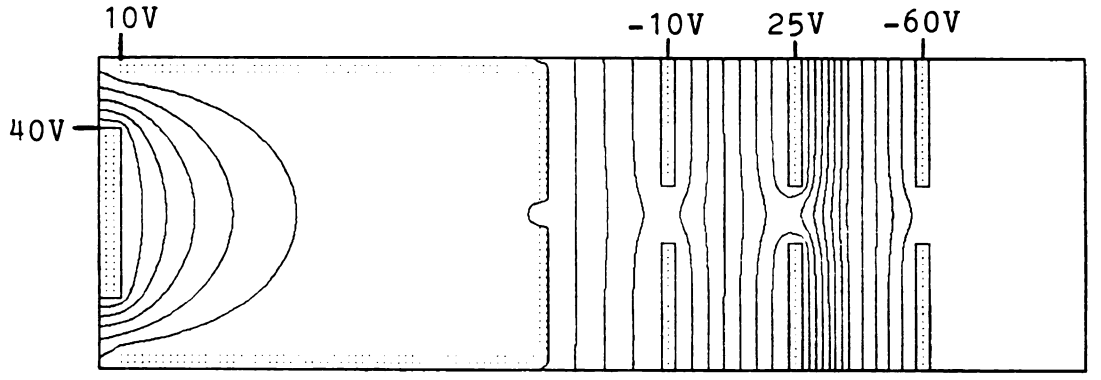

Figure 3-3. The equipotential map of the ion source and lenses in Figure 3-2.

parts by segmenting the chamber at some longitudinal position on the cylindrical wall. These two parts are the repeller which consists of a plane and a cylinder, and the ion exit which consists of a plane with a small hole in the center, with or without a cylinder.

Table 3-1 and Table 3-2 present the regions from which ions formed with no initial translational energy will pass the chamber exit for a variety of ion source designs. Table 3-1 shows that ion source design numbers two (2) to twelve (12) provide longer stable regions for ions to pass through the source exit than does the first (the original) design. Design two has the same configuration as the first design but has a higher voltage on the repeller. This design shows a little longer stable region. Designs 3, 4, 5, 6, 8, 10, 11 and 12 have the same repeller voltage as the first design but vary in the repeller shape.

Table 3-1. Stable regions for ions formed in several source designs, at different x values with the same y value of 0, to pass the source exit.

No.	Design	x
1	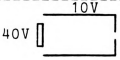	0 - 22
2	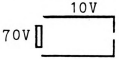	0 - 28
3	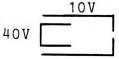	0 - 42
4	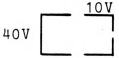	0 - 42
5	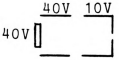	0 - 42
6	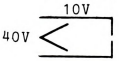	2 - 40
7	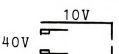	0 - 36
8	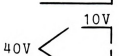	2 - 42
9	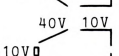	16 - 44
10	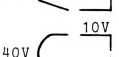	0 - 42
11	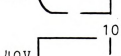	0 - 54
12	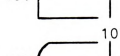	0 - 54

Table 3-2. Stable regions for ions formed at different positions to pass the source exit in different ion sources. (Blank space represents no stable region.)

Design No.	±Y								
	X = 1	6	11	16	21	26	31	36	41
1	0	0	0	0					
2	0	0	0	0	0	0			
3	1	1	1	1	1	3	0	0	0
4	4	3	3	3	7	2	1	0	0
5	4	3	3	3	6	2	1	0	0
6		2	1	1	2	2	0	0	
7	2	1	1	1	3	0	0	0	
8	0	1	1	4	7	1	0	0	0
9					1	5	1	0	
10	2	2	2	2	3	4	2	0	0
11	4	3	3	2	2	1	2	2	2
12	4	3	3	2	2	2	2	2	2

Table 3-2 shows that different ion source designs have different widths of stable regions. The first and the second designs have the same width of stable region because they have the same configuration. Ion source designs 3 to 12 show a large increase in the stable region because the shapes of their repellers produce a focusing electric field, and therefore sample from a larger volume.

The total solid volume of stable region for ions to pass through the source exit is used for preliminary comparison of ionization efficiency. The total solid volume is approximately the sum of all individual solid volumes which are formed by dividing the total solid volume into equal interval slices along the x-axis. The solid volume of each slice can be approximately calculated by the equation $V = l\pi r^2$, where V is the volume, l is the interval length, r is the radius of the stable region at that slice which is expressed as a y value, in units of 0.032 cm. A volume unit is the cube of the unit length and has a value of 3.2×10^{-5} cubic centimeter. In Table 3-2, the interval of 5 length units is chosen to calculate the approximate total solid volume. For example, design 3 has a volume of 220 units and design 4 has a volume of 1500 units.

Effective Sampled Volume

Table 3-3 gives the results of the studies of stable regions of several ion source designs in more detail. Generally, the volume in which ions are formed in many mass spectrometers is only part of the total source volume as is the volume from which formed ions will exit the source. The effective sampled volume in an EI source of a mass spectrometer is also determined by the volume of the electron beam. The electron entrance slot in our source is

Table 3-3. Detailed stable regions of some ion source designs for forming ions to pass the exit. (Blank space represents no stable region.)

Design No.	±Y								
	X = 0	2	4	6	8	10	12	14	16
1	0.7	0.6	0.4	0.3	0.2	0.2	0.2	0.2	0.2
4	5.0	4.1	3.4	3.0	3.0	3.0	3.0	3.0	3.3
10	2.2	2.0	2.0	2.0	2.0	2.0	2.0	2.1	2.2
11	2.8	3.3	3.5	3.5	3.3	3.2	3.0	2.9	2.7
12	3.8	4.3	3.6	3.5	3.4	3.2	3.1	2.9	2.7

Design No.	±Y								
	X = 18	20	22	24	26	28	30	32	34
1	0.1	0.1							
4	4.0	6.0	8.1	4.0	2.7	2.2	1.6	0.9	0.9
10	3.0	3.3	4.1	7.0	4.9	2.8	2.3	1.7	1.0
11	2.6	2.4	2.2	2.0	1.9	1.9	2.0	2.0	2.0
12	2.6	2.4	2.2	2.0	2.0	2.0	2.0	2.1	2.1

Design No.	±Y									
	X = 36	38	40	42	44	46	48	50	52	54
1										
4	0.8	0.8	0.9	0.9						
10	0.9	1.0	0.9	0.9						
11	2.0	2.0	2.1	3.1	7.9	4.7	3.5	1.7	1.3	1.1
12	2.1	2.1	2.2	3.0	7.9	4.6	3.5	1.7	1.3	1.1

about 25 length units long and 5 length units wide. The shape of the ionization electron beam, the ionization volume, is a rectangular box. The effective sampled volume (the volume where ions can both be formed and exit the source), is the three-dimensional intersection of the stable region and the ionization volume. Consider first the two extreme cases. When the stable region is narrower than the width of the ionization volume, the effective sampled volume can be approximately calculated by the method described before, with the first equation $V = l\pi r^2$. When the width of the ionization volume is narrower than the stable region, the effective sampled volume of each slice can be approximately calculated by the second equation $V = 2wlr$, where w and r are the width of the ionization beam and the radius of the stable region at that slice. The effective sampled volume of each interval slice along the x-axis is the individual intersection of the stable region and the ionization volume at that slice and can be approximately calculated by either the first or the second equation, whichever is more appropriate. The effective sampled volume for the source is the sum of the effective sampled volume of all slices.

On this basis, the approximate effective sampled volume can be calculated, and the relationship between design one and others can be compared. The region which is taken into account for the comparison of ionization efficiency includes

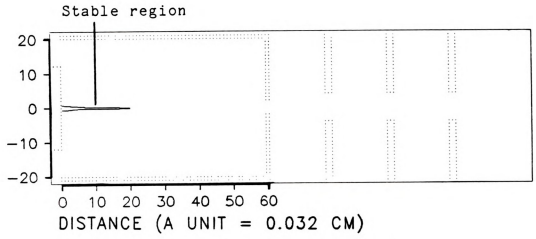

Figure 3-4. The stable region in the ion source used in our mass spectrometer for forming ions to pass through the source exit.

the x values beginning from 18 to 42. The actual sampled volumes of designs 1, 4, 10, 11, and 12 are 0.126, 600, 527, 404, and 420 volume units respectively.

Figure 3-4 shows that the stable region for forming ions with trajectories passing through the exit of the original ion source is just a very narrow and short region. Ions formed outside this region will not exit the source. This stable region is almost on the line between centers of the front of the repeller and the exit slit.

Figure 3-5a shows the shape of the ion source in design 4 and some trajectories of ions formed in this source. As shown, ions formed at many different positions inside the ion chamber will be accelerated and focused to pass the exit of the chamber. Figure 3-5b shows the equipotential map in

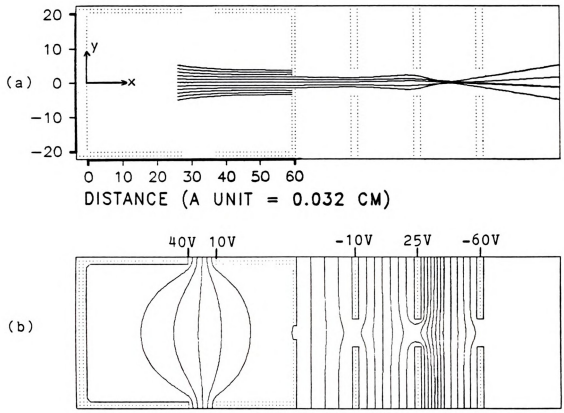

Figure 3-5. (a) The shape of the ion source in Design 4 and some trajectories of ions formed in this source. (b) The equipotential map for the ion source and lenses in this design.

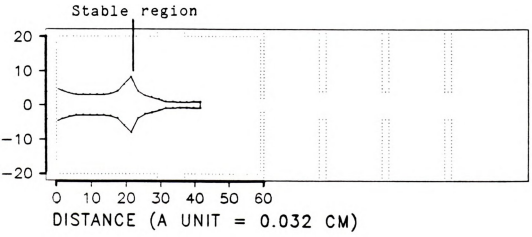

Figure 3-6. Schematic representation of the stable region for forming ions to pass the source exit of the source design in Figure 3-5.

the ion source and among lenses of this design. This figure reveals that the concave equipotential lines at the left side of the segmentation bring about focusing force to the ions in the ion chamber and produce significant improvement of ionization efficiency in the ion source.

The possible sampling volume in this ion source of design 4 was plotted in Figure 3-6. The regions for forming useful focused ion current have been greatly enlarged over the normal repeller design in all three dimensions. Figure 3-7 shows the same ion source with increased transmission of ions due to an increase in the exit aperture. With flat planes on both ends of the repeller and the ion exit plate, this ion source can be made in the shape of a cylinder.

Figure 3-8 shows another design (Design 11) of the ion source and the schematic drawing of stable region in the chamber for forming ions to pass the exit. This design has a segmentation just behind the exit plane of the source.

As shown in Figure 3-9a (Design 12), the repeller has been designed with the combination of a round concave part and a cylindrical part. The segmentation in the ionization chamber is just behind the exit aperture plate which now has the shape of a lens. The stable regions for ions formed in this ion chamber to pass the exit slit are shown in Figure 3-9a. Figure 3-9b shows the equipotential map of this source. The concave equipotential lines show the focusing electric field for producing high ionization efficiency.

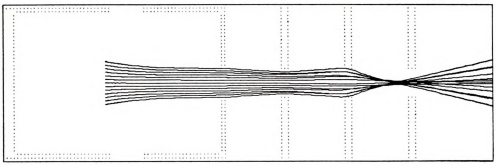

Figure 3-7. Ion trajectories in an ion source with a larger exit aperture than that shown in Figure 3-5.

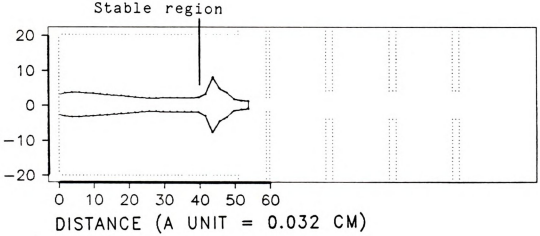

Figure 3-8. The shape of an ion source design and the stable region in this source for forming ions to pass the source exit.

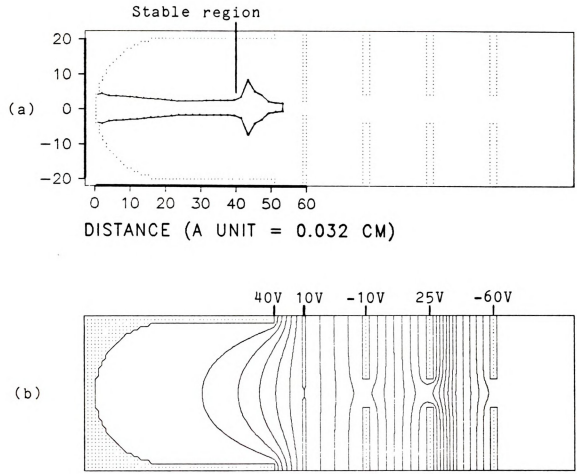

Figure 3-9. (a) The shape of an ion source design and the stable region in this source for forming ions to pass the source exit. (b) The equipotential map of this source.

According to design 12, the electron inlet can be a slot with x values beginning from 18 to 42 on the bottom of the chamber. This configuration has inside dimensions of 60 and 40 for x and y values. This ion source has a simple ratio of 3 to 2 for the x and y dimensions and can be made with an x-axis length 1.9 cm, y-axis length 1.25 cm, with an electron inlet a slot 0.8 cm long in the middle of the cylinder wall. This source would be constructed in the shape of a cylinder witha hemispherical base as the repeller part, looking from both inside and outside the chamber.

Ion Energy Spread

The original ion source and the other source designs described above have about 11 eV of kinetic energy spread when used with the same electron entrance slot. In order to decrease the spread in ion kinetic energy spread from the source, another ion source design is proposed.

Figure 3-10a shows this source. The source has three parts consisting of the repeller, the body, and the extractor and exit aperture. The length of this source is the same as that of previous designs, but the height of it is half of that of previous designs. The lens system is kept the same. The front center of the repeller is assigned as the origin. Figure 3-10a also shows the stable region in this source. Figure 3-10b shows the equipotential map of

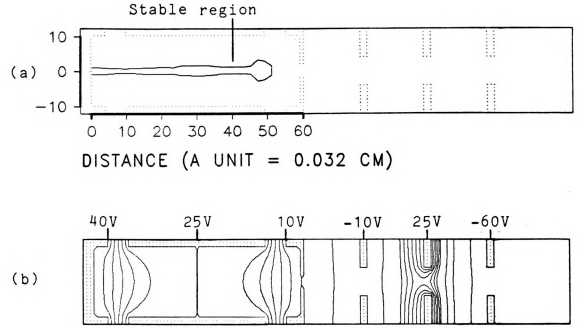

Figure 3-10. (a) The ion source which will produce ions of small kinetic energy spread and the stable regions in this source. (b) The equipotential map of this source.

this source. The equipotental map shows that there is a long range with little potential gradient in the intermediate part. Limiting ionization to this region results in the small spread in the ion kinetic energy.

Table 3-4 shows the detailed study of the stable region for ions formed in this source to pass through the exit. By using the first equation for calculation, the actual sampled volume of this ion source is 110 volume units. This source will produce focused ion current 880 times higher than the original source does.

Table 3-4. detailed useful regions of the ion source which will produce ions of very small kinetic energy spread.

X	0	2	4	6	8	10	12	14	16
±Y	1.0	1.0	0.9	0.8	0.7	0.6	0.7	0.8	0.9

X	18	20	22	24	26	28	30	32	34
±Y	0.9	1.0	1.0	0.9	1.4	1.4	1.5	1.5	1.4

X	36	38	40	42	44	46	48	50	52
±Y	1.2	1.0	1.0	1.0	1.0	1.1	3.0	2.7	1.3

Figure 3-11 shows the relationship between ion's kinetic energy at the chamber exit and the distance from the origin to the place where ions were formed. This figure shows a flat region beginning from distance units 18 to 42. Ions formed in this region will have a small kinetic energy spread, with a maximum of about 4 eV. If an even smaller energy spread is desired, the electron entrance slot can be reduced to distance units 26 to 41. This will give an ion kinetic energy spread of less than 2 eV without too much sacrifice in ionization efficiency. The calculated sampled volume in this source is 86 volume units and is still 680

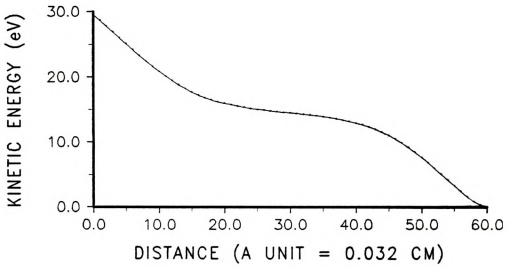

Figure 3-11. Relationship between ion's kinetic energy (eV) at the chamber exit and the distance from the origin to the place where ions were formed. Mass = 40 (M/z). Initial ion kinetic energy = 0 eV.

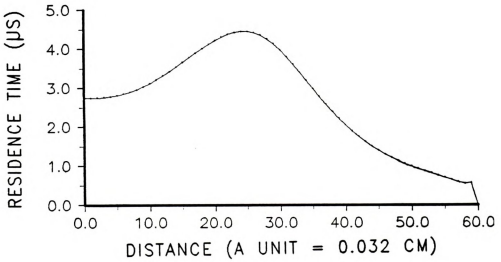

Figure 3-12. Relationship between ion's residence time (μs) in the source and the distance from the origin to the place where ions were formed. Mass = 40 (M/z). Initial ion velocity = 0 cm/sec.

times larger than that in the original source. In addition, the source volume is smaller and will provide more effective use of the sample.

Figure 3-12 shows the relationship between ion's residence time in this ion source and the distance from the origin to the place where ions were formed. The peak in the range of distance units 10 to 35 shows that ions formed in this range have longer residence time. This phenomenon is caused by the long range of small potential gradient in the intermediate part. Ions formed in this part thus will have smaller initial velocities. This study illustrates the factors and compromises involved in trying to achieve high efficiency, low energy apread, and short residence times in ion source design.

Conclusions

Significant improvements in ion source efficiency and overall performance for mass spectrometry using EI modes can be achieved by computer simulation without alteration of the exit lens system. The four computer-aided ion source designs can produce focused ion current three thousand times higher than the ion current produced by the ion sources most commonly used. It's use would be expected to increase significantly the total sensitivity of the triple quadrupole

mass spectrometer.

A new ion source has been designed by computer simulation which will provide a very low ion kinetic energy spread (less than 2 eV). Ion focussing maintains efficiency several hundred times higher than the simple repeller type ion sources.

CHAPTER 4

COMPUTER-AIDED LENS SYSTEM STUDIES AND ION PATH BENDER DESIGNS

Introduction

Ion lenses have been widely used in many mass spectrometers. They are placed between the source and the analyzer, and between the analyzer and the detector to control the ion path for better transmission. The design of lens elements and the determination of an optimal combination of voltages on all lenses are a combination of an art and the science of ion optics.

Giese [32] developed an electrostatic quadrupole lens as a strong focusing ion source for mass spectrometers. Lu and Carr [33] studied the focusing properties of a quadrupole lens pair. Under the special conditions that the ion beam entering the lens system is rectangular and the exiting beams are parallel and in one plane, they derived equations of a quadrupole lens pair for a mass spectrometer using ribbon-shaped ion beams. Loveless and Russell [34] used trajectory calculations to design a new electrostatic lens with strong-focusing properties for a surface ionization ion source. Recently, Winkler and Beckey [35] presented an ion optical system with high transmission for

field ionization/desorption (FI/FD) source. Read et al.[36] studied a method of solving Laplace's equation for electrostatic cylinder lenses of two element system.

Natali et al.[37,38] developed methods for calculations of properties of the two-tube electrostatic lenses. Fink and Kisker [39] developed a method for rapid calculations of electron trajectories in multi-element electrostatic cylinder lenses. Shortly thereafter Kisker [40] published a short BASIC program for calculating electron and ion trajectories in multi-element tube lenses.

Up to now the use of a lens system to bend ion paths for eliminating the neutral molecule interference in mass spectrometry such as TQMS has not been discussed. In this chapter, the effects on the stable ion paths by the aperture, the thickness, and the angle of each lens, and the distance between adjacent lenses or between the source chamber and the lens will be discussed. The experimental section describes the procedure for computer simulation studies in lens system. The importance of finding the optimal combination of voltages on lenses also will be discussed. By using computer simulation, three designs of lens systems to bend ion paths for eliminating neutral molecule interference in TQMS and a design of inter-quadrupole lens system to increase the transmission will then be discussed.

Experimental

A computer simulation method was used to calculate the ion trajectories in different lens systems. The computer program used was described in previous chapters. For studying the effects of lenses on the transmission of ions from the source, the electric field was constructed to include the source and lenses. Ions were placed at different positions in the source with zero initial kinetic energy. Under the electrostatic field, increments of the ion motion were calculated and the ion trajectories observed. The first study was the source and lens system which was the commercial unit first used on our mass spectrometer [2]. The parameters studied were the aperture, the thickness, and the angle of the lens, the distance between lenses, and the voltage applied to the lens elements. Keeping others constant, one parameter was varied to study its effect on the transmission from the source to make the exit of the last lens. In studying the effect of voltage, the voltage on a lens was varied at a time while the voltages on other lenses were constant. From this voltage study, an optimal combination of applied voltages can be found.

In designing the ion bender, different types of lenses were "built" by the computer program with several trials of applying different combinations of voltages. Ion

trajectories in the lens system are found to be independent of mass to charge ratio. Trajectories were studied for ions entering with the same direction or with many different directions, and with a same initial kinetic energy. The performance of each design was then studied. Taking into account the effects of the aperture, the thickness, the distance, and the angle, an inter-quadrupole lens system was designed.

Results and Discussion

Source Lens System

The computer simulation method was used to study the effects of parameters on the lens system, the design of the lens sytem for ion path bender, and the design of an inter-quadrupole lens system. Figure 4-1 shows the configuration of the ion source and lens system first used on our mass spectrometer. In order to study the effects of the parameters of lenses, the front center of the repeller was assigned values of 0 on the x and y spatial coordinate. The x value of the center of the ion source exit was assigned as 60, and the y value of the inner top of the ionization chamber was assigned 20, with unit length of 0.032 cm. The three lenses were labeled as A, B, and C for the purpose of voltage study. The labels a, t, and d

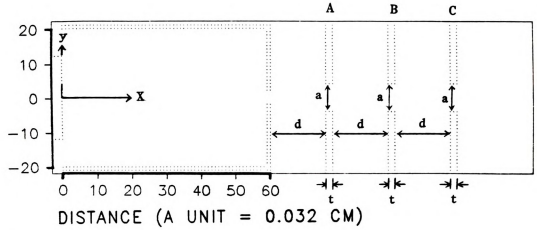

Figure 4-1. The configuration of the ion source and lens system first used on our mass spectrometer. The front center of the repeller is assigned as the origin. Three lenses are labeled as A, B, and C. The symbols a, d, and t are the aperture, the distance, and the thickness of the lenses, respectively.

represent the aperture, the thickness of the lens, and the distance between lenses or between the lens and the source chamber.

Table 4-1 shows the effects on the ion transmission by the voltage on each lens. Column 2, 3, and 4 are the voltage on each lens. Column 5 is the stable region where ions formed can get out of the source and pass all the lenses. The stable regions were studied for a y value of 0 with different x positions. The voltages on the repeller and on the source chamber, 40 and 10 V, respectively, were first used with our mass spectrometer. Trial 1 used the voltage values first used for our TQMS and will be used as the standard setting for the comparison with other trials.

Table 4-1. Effects of voltage of the lens system on ion's transmission.

No.	A (V)	B (V)	C (V)	X Stable Region at Y = 0
1	-10	25	-60	0 - 20
2	-10	10	-60	0 - 60
3	10	25	-60	0 - 4
4	-10	25	10	0 - 12
5	10	25	10	0 - 2
6	10	10	10	0 - 58

* A, B, and C represent lenses A, B, and C.

The result showed that the stable region begins from distance units 0 to 20.

Trial 2 had a different voltage on lens B but the others were kept constant. This value of 10 V was the same as that of the ion chamber. This combination of voltages dramatically increases the stable region from the range of distance units 20 to 60. The reason for this big increment is that the 25 V on lens B in Trial 1 was a high energy barrier for ions to pass, but the 10 V on lens B in Trial 2 decreased the energy barrier for ions by 15 V, and actually the energy barrier was removed completely. Trial 3 placed 10 V on lens A. This trial showed a sharp decrease on the stable region from the range of distance units 20 to 4. The increase of the voltage on lens A from -10 V to 10 V caused

the loss of the accelerating force that lens A had when it was -10 V.

Trial 4 used 10 V on lens C and showed a decrease in the stable region from the range of distance units 20 to 12. The 10 V on lens C lost the attracting factor which the -60 V on lens C provided. Trial 5 showed even lower transmission with a smaller stable region by losing the accelerating force, or attractive force, or both, compared with Trials 4, 3, and 1. But with the decrease of the voltage on lens B from 25 V to 10 V, the stable region increased sharply with the range beginning from distance units 2 to 58 which was very close to the maximum value of distance unit 60 obtained in Trial 2. This Table revealed the importance of the voltage and of finding an optimal combination of voltages on the lens system. It also provided some understanding of the effects of voltage on the lens sytem and the stable region for ions formed in the ion source.

Table 4-2 shows the effects of the aperture, the thickness of the lens, and the distance between lenses or between the lens and the source chamber on the transmisson of ions. The symbols d, t, and a in column 2, 3, and 4 represent the distance, the thickness, and the aperture, respectively in cm. Column 5 represents the stable region of ions formed at the same value of y but different values of x. Trial 1 gave a stable region beginning from distance

Table 4-2. Effects of the aperture (a), the thickness (t), and the distance (d) of the len system on ion's transmission.

No.	d (cm)	t (cm)	a (cm)	X Stable Region at Y = 0
1	0.51	0.06	0.25	0 - 20
2	1.02	0.06	0.25	-
3	0.51	0.03	0.25	0 - 25
4	0.51	0.06	0.12	0 - 5

units 0 to 20 with d, a, and t values first used on our mass spectrometer. This will be used as the standard set for comparison with the other settings. In trial 2 the distance doubled and the other parameters remained constant. It showed no stable region for the ions formed in the source. This showed that the distance played a very important role on the transmission of ions. As the distance decreased, the transmission increased.

Trial 3 used a thickness of half the value with other parameters kept the same. It showed a small increase on the transmission by increasing the stable range from distance units 20 to 22. Trial 4 halved the value of the aperture on each lens with other values kept constant. It showed a remarkable decrease in the ion transmission by shortening

the range of the stable region from distance units 20 to 5. Therefore, it was recommended from this study that one can increase the aperture of the lens, decrease the thickness of the lens, decrease the distance, or two or all of them in order to increase ion transmission thus the sensitivity of the mass spectrometer.

Ion Path Bender

In order to eliminate the neutral molecule interference in TQMS, three ion path benders were designed by computer study. Figure 4-2 shows the first of the bender designs. In this bender design, a pair of curved lenses were used as the bender and placed between the left and the right lenses. The voltages on this pair of curved lenses were different. A positive voltage was on the bottom one, and a more positive value on the top one. The angle between the left and the right lenses was 20 degrees. The voltages on the left and on the right lenses had the same values which were less positive than the voltages on the curved lenses. The pair of curved lenses provided bending and focusing effects. The right lens provided the guiding effect to make the exiting ions with smaller divergence. Ions entering the left lens with parallel direction and with the same initial kinetic energy were focused to the center of the lens exit. Ion paths leaving the lens exit were bent about 20 degrees

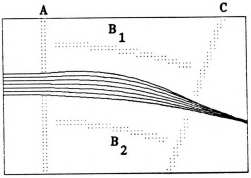

Figure 4-2. The first ion path bender design. The angle between lenses A and C is 20 degrees. The voltages on lenses A, B_1, B_2, and C are 0, 10, 7, and 0 volts, respectively.

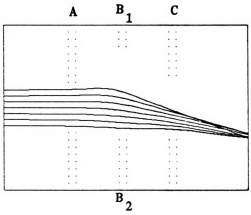

Figure 4-3. The second ion path bender design. The voltages on lenses A, B_1, B_2, and C are 0, 8, 0.5 and -3 volts respectively.

with respect to the direction of entering ions. This design showed the effects of bending in addition to focusing and centering.

Figure 4-3 shows another design for the ion path bender with three parallel lenses. In this design the central lens provided the bending characteristics. This lens was separated into upper and lower pieces with different voltages on them. The bottom part of the central lens had a small positive voltage and the top part had a larger positive voltage value. These two parts provided bending and focusing effects. The desired bending degree can be adjusted by changing the voltages on these two parts. The third lens had a negative voltage to guide the leaving ions with less divergence.

Figure 4-4 shows the best design for the ion path bender. In this Figure, the left-most part was the ion source exit. The right-most part represented the ELFS. The ELFS is a cylindrical aperture made from a leaky dielectric material. The ELFS on our mass spectrometer was obtained from Extranuclear Laboratories. It shields the ions from the DC fields while not fully shielding them from the RF field. It was installed in our mass spectrometer to reduce the effects of fringing fields of the quadrupole and thus offered improvement in the transmission of the ions. The two lenses are in the middle of Figure 4-4. The first lens has a more positive voltage than the source exit and thus

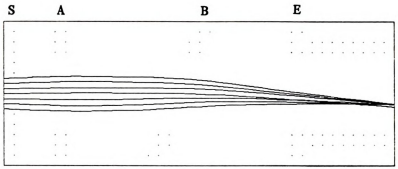

Figure 4-4. The third ion path bender design. A and B are lenses. S is the source chamber and E is the ELFS. The voltages on S, A, B, and E are 10, 14, 14, and 5 volts, respectively.

provided the focusing effect. The second lens has the same voltage as the first lens. This lens was a whole piece and had an angle of 20 degrees with respect to the first lens. It bent the ion path about 2 to 5 degrees as was our desire. The degree of bending can be adjusted by changing the voltage on the second lens (the bending lens). The right-most part (ELFS) had a lower voltage than the second lens. It provided also the guiding effect to make the ion paths parallel and focused. This part could be assembled at the same desired angle with respect to the direction of original ion paths but parallel to the exiting ion paths.

The first design of the ion path benders used a pair of curved lenses. The preparation and the installation of this lens pair could be difficult. The second design used three

parallel lenses. It needs less space. The central lens was actually two pieces with different voltages. The third design is the best design for ion path bending. There are only two lenses, one serving focusing effect, the other one serving bending effect. The ELFS is another part of the instrument serving the guiding effect. The bending lens is a whole piece. The preparation and the installation for this design are relatively simple. This design is under construction in our mass spectrometer to eliminate the interference of neutral molecules.

Figure 4-5 shows the combination of a new ion source design and a new lens system design. The new source designed by computer simulation has been described in Chapter 3 and provides a high ion current. This new lens system provides focusing, bending, and guiding properties. The first lens had two different voltages on the two separated pieces. The top piece had a lower positive voltage than the source exit does. The bottom piece has a even lower positive voltage. These two pieces provide the bending and the guiding effects. The second lens had a higher voltage than the first lens. This provides the focusing effect for the ion paths.

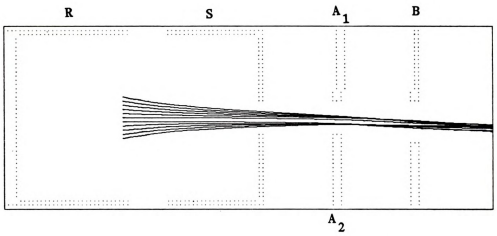

Figure 4-5. The combination of a new ion source design and a new lens system design. A_1, A_2, and B are lenses. R is the repeller and S is the source chamber exit.

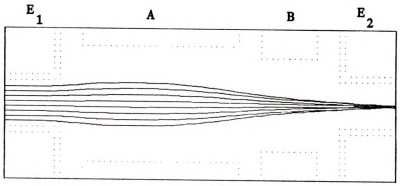

Figure 4-6. An inter-quadrupole lens design. E_1, and E_2, are ELFS. A and B are lenses. The voltages on E_1, A, B, and E_2, are 0, 10, -10, and 0 volts, respectively.

Inter-quadrupole Lens System

Figure 4-6 shows an inter-quadrupole lens system design. The left-most part and the right-most part are the ELFS fitted into the quadrupoles to remove the fringing field effect. They were assigned the same voltage. The two lenses are between the two ELFS. The first lens has a higher voltage than the left ELFS. It provides the focusing effect. The second lens has a lower voltage than the first lens and the ELFS. It provides the guiding effect for the ion paths to become parallel and centered. This design has been constructed in our mass spectrometer and shown experimentally the increase of sensitivity for ions of high mass to charge ratio up to a factor of ten.

Conclusions

Understanding the voltage effects or using a computer to select values for the parameters will provide a good means to find the optimal combination. Improved transmission is achieved with increased aperture of the lens, decreased thickness of the lens, and decreased distances between adjacent lenses or between the source chamber and the lens. Practical considerations including the proper function for the lens system and no electric break-down, will determine the maximum value for the

aperture and the minimum value for the thickness and distances.

The implementation of an ion path bender should eliminate the problem caused by the neutral molecule interference in TQMS. All three designs should work well. They all provide bending, focusing, and guiding effects.

The design of the inter-quadrupole lens system presents a significant improvement in the instrumentation. The installation of this lens system in our mass spectrometer shows an experimental increase in sensitivity for ions of high mass to charge ratio up to a factor of ten. This demonstrates the value and significance of computer simulation studies of the ion path.

CHAPTER 5

COMPUTER SIMULATION PROGRAM

Description of Program

The computer program uses digital simulation for studies of ion (electron) trajectories. It was developed by D.C.McGilvery in J.D.Morrison's laboratory, Department of Physical Chemistry at Latrobe University in Australia. It was written in Fortran IV, and the plotting subroutine was written in Assembly language. McGilvery and Morrison used it to calculate the ion trajectories, distributions, and densities in the central quadrupole of their tandem quadrupole mass spectrometer for the study of laser-induced photodissociation of ions [8]. R.A.Yost and C.G.Enke used this program to calculate ion trajectories in the RF-only central quadrupole of our triple quadrupole mass spectrometer system [4].

The program has been modified to fit our current PDP 11/40 minicomputer RSX-11M multiuser operating system [19] with 128K words of memory cartridge disk, Tektronix graphics terminal, and Printronix graphics printer or Versatec graphics printer. The plotting subroutine is now changed to Fortran IV. Some functions have been added to allow the selection of graphics terminals, to change the quadrupole

length, to perform different types of ion trajectory studies in a single run, and to provide adjustable physical dimensions. This program utilizes an overlay structure and requires 32K words of memory.

Functions of Program

The main program controls the selection of functions and provides the setup of the plotting parameters. Ten functions are available in this program including Old, Save, New, Modify, Refine, Contour, Trajct, Qtrag, Qtrajf, and End. In the main program, the terminal for plotting has been assigned. The plotting parameters of x and y margins, x minimum and x maximum numbers of plotting points, y minimum and y maximum numbers of plotting points are set automatically by the program. The lengths for x-axis and y-axis are determined by the user.

The option "Old" reads from the computer memory a file of specified name previously created by the program. The file contains an array of up to 5000 points of the potential of a plane through an electrode configuration. It is stored in binary code. In reading this file, if error occurs or the reading finds the end of file, messages will be given to the user.

The option "New" sets up a new potential array and the electrode configuration. The name should be specified and

dimension of the array decided. The file is written in binary code for quick writing and reading and for saving the space of the memory. The messages will be sent out in case of error in writing or end of file.

Subroutine "Modify" allows the current array to be modified, potential changed, and electrode altered. This subprogram enables the user to build the electrodes with different shapes and different potential values. A circular electrode can be built by specifying its central coordinates of x and y values, its radius, the value of its potential and by specifying it an electrode. A rectangular electrode can be built by specifing the lower left x and y coordinates, x length, y length, and its potential, as well as marking it an electrode. Electrodes of triangular shape, or point electrode, or block change, can be accomplished by a similiar mechanism. This subroutine clears the graphics terminal, and plots the electrode configuration, or creates a file for hard copy of this configuration.

The "Refine" subprogram interatively refines the potential to calculate all non-electrode potentials. Between 100 and 1000 iterations are usually required in the trajectories. The refinement factor and the limit of error correction can be specified. A high accuracy can be reached up to one part in ten billion for the error limit. If the sum of the changes in potentials of all the points altered during that iteration is less than the specified limit, or

if the number of iteration is reached, this subroutine prints the sum of the changes at the final iteration, and control returns to the main program.

The subroutine "Contour" draws an equipotential contour map of the current potential array. It clears the plotting terminal and draws the electrodes or creates a file of this map. By scanning through the pre-constructed potential array, this subroutine finds the potential on four points surrounding a certain place, and then calculates intercepts of each contour by these four points and the sides of them. After drawing the contour line segments, this subroutine returns to the main program.

Subroutine "Trajct" allows a series of ion (electron) trajectories to be calculated in electrostatic mode and to be plotted, and data on focii and residence time is printed. Trajectory calculations are based on elementary equations in classical physics. After reading the "Old" file, this subroutine contains the potential array which consists of electrodes and non-electrodes. Ions can move in the space of non-electrode under the force of electrodes. The acceleration was produced on the ion of m/z by the electric field at t = 0. The acceleration is calculated by the equation $F = ma = zE$. When the time interval is small enough, the acceleration can be considered constant over that interval. The simple kinetic energy equation KE = 0.5 mv^2 is used. Trigonometric functions of sine, cosine, and

tangent are also used. The initial position, energy, direction, and the m/z of the ion are input by the user. The space of the configration, the voltage scale, and the number of calculation are determined at the beginning of running this subroutine. This subroutine calculates the initial x and y velocities. Then it finds potentials of 4 points surrounding that ion, calculates potential gradients, the force, new velocities, new energy, and the new position. The trajectory of each calculation is plotted for each step. When the ion reaches the boundary or the electrodes, the final trajectory is plotted. The final position, energy, direction, and the time of flight of the ion are printed.

Subroutine "Qtrajf" is based on the same concept of trajectory calculations as that in subroutine "Trajct", except that the dynamic field mode is used. A data file of the list of sine functions is read from the memory. The electric field is changing from time to time according to the sine wave function thus changes the acceleration force. The force, new velocities, and the new positon of an ion are calculated by finding the potentials on 4 points surrounding the ion and calculating the potential gradients. The space of the configuration, the RF frequency, and the peak voltage are input for experimental situations. The other needed values include the ion's m/z ratio, position, off-axis energy, radial angle with respect to x-axis (assuming the axis of quadrupole is z, the axes of quadrupole cross

section are x and y), the axial energy, the quadrupole length, the diameter of the exit orifice, and the number of wanted trajectory calculations. The time resolution is one hundredth of one period of the RF field variation. The time needed to pass the quadrupole and time of flight are calculated for finding the stability of the ion. In the investigations of effect of fragmentation in the collision chamber, m/z of the fragment ion and time of its fragmentation are supplied.

Subroutine "Qtrag" has the same principles and functions as subroutine "Qtrajf". The only difference is that the position of fragmentation instead of fragmentation time is supplied for studying effects of fragmentation.

The plotting subroutine was originally written in Fortran IV by Dr. Thomas Atkinson and uses "Vector" as its subroutine. It has been modified to add functions of initiation, continuaction, and termination of plotting and the function of drawing factor which provides selection of moving the cursor, plotting surface at the beginning and draws dots or lines for succeeding calculations.

A separate small program "Table" creates a file of the table for sine wave function. One hundred steps have been used for each computation cycle of a sine wave. In the calculation of ion trajectories in an electric field which is changing dynamically, double precision utilized for this table provides more accurate results.

CHAPTER 6

FUTURE RESEARCH

Computer simulation studies of ion trajectories provides a good way to understand the behavior of ions in TQMS and the characteristics of TQMS system. A number of new designs and guidelines for improvement in operation and application have been obtained. The theoretical study of the inter-quadrupole lens design has been implemented and the resultant transmission of high mass to charge ratio has been increased by a factor of ten. An ion path bender design is under construction for our mass spectrometer. A new EI ion source construction is under consideration taking advantages of computer-aided design. The understanding of ion behavior through the quadrupole has been applied to improve the choice of settings for the quadrupole system.

Several future topics for research and instrument improvement are recommended. Computer simulation study of an RF-only quadrupole mass filter can be extended to study systems with more than four poles. Some multipole systems are under investigation. A thorough investigation of them promises interesting results. A high efficiency ion source with small energy spread is desirable for an EI source and is under consideration for testing. Computer simulation of a CI source and an FI/FD source were tested and are subject

to further exploration. The detector system is also an interesting area for research. Simulation studies for mass spectrometry with electric sector and its lens system, for time of flight (TOF) mass spectrometry, for ion cyclotron resonance (ICR) mass spectrometry and other types of mass spectrometry are advisable.

The computer program can be modified to include more sophisticated functions. A program could be added which will construct an arc of a circle with a certain range of angle and a certain range of length for electrode. This will enable simulation studies on the electron multiplier. Utilization of the university computer system will improve the limitation of memory size in the minicomputer system and will provide much higher calculation speed.

It is desirable to take advantages of the results from computer simulation studies of ion trajectories in TQMS, ie, effects of the RF peak voltage, frequency, the r/r_o ratio, the high efficiency ion source which will produce ions of very small kinetic energy spread, the ion path benders, and the inter-quadrupole lens system, to develop a more ideal TQMS instrument.

Computer simulation studies in TQMS system offer many advantages. The computer simulation methodology shows from the results that it is a powerful tool for theoretical calculations, instrumental design, and analytical applications. Its capability reveals its significance not

only for the present work but also for wide applications in future research.

APPENDIX

```
C       PROGRAM SIMION
C
C       THIS IS THE MAIN CONTROL PROGRAM FOR THE ION SIMULATION
C       PROGRAMS DEVELOPED AT LATROBE UNIVERSITY ,DEPT. PHYS. CHEM.
C       BUNDOORA VIC. AUST. 1977. VERSION 1. BY D. C. MC GILVERY,
C       AND MODIFIED AT MICHIGAN STATE UNIVERSITY, DEPARTMENT OF
C       CHEMISTRY, MARCH 1980, BY JIIN-WU CHAI.  THE PROGRAMS
C       ARE WRITTEN FOR A PDP11 RSX-11 MULTIUSER SYSTEM, UTILIZING
C       AN OVERLAY STRUCTURE AND 32K MEMORY IS REQUIRED.  AN ARRY
C       OF UP TO 5000 POINTS CONTAINS THE POTENTIALS OF A PLANE
C       THROUGH AN ELECTRODE CONFIGURATION.  3 SYMMETRIES ARE
C       AVAILABLE (A) PLANAR WITH A SYMMETRY AXIS ALONG THE X AXIS,
C       (B) PLANAR  WITH NO AXIS OF SYMMETRY(THESE ARE ADEQUATE FOR
C       3-D REPRESNTATIONS OF SLIT LENS SYSTEMS, ETC.)
C       3 (C) CYLINDRICAL SYMMETRY (CYLINDER AXIS ALONG X AXIS)
C       OPTIONS AVAILABLE IN THIS PROGRAM.
C       1.OLD - READS FROM UNIT 2 A FILE OF SPECIFIED NAME PREVIOUSLY
C       CREATED BY THE PROGRAM.
C       2.SAVE - WRITES ONTO UNIT 2 A FILE OF SPECIFIED NAME OF THE
C       POTENTIAL ARRAY CURRENTLY IN CORE.
C       3.NEW - SETS UP NEW POTENTIAL ARRAY & ELECTRODE CONFIGURATION
C       4.MODIFY - ALLOWS THE CURRENT ARRAY TO BE MODIFIED, POTENTIALS
C       CHANGED, AND ELECTRODES ALTERED.
C       5.REFINE - ITERATIVELY REFINES THE POTENTIAL ARRAY TO CALC. ALL
C       NON ELECTRODE POTENTIALS.
C       6.CONTOURS - DRAWS AN EQUIPOTENTIAL CONTOUR MAP OF THE CURRENT
C       POTENTIAL ARRAY.
C       7.TRAJECTORIES - ALLOWS A SERIES OF ION(ELECTRON) TRAJECTORIES
C       TO BE PLOTTED ,DATA ON FOCII AND RESIDENCE TIME IS PRINTED.
C       8.END - ENABLES THE USER TO GET BACK TO MONITOR !!!!!!!!!.
C
        BYTE IO,OLD,SAV,MOD,REF,TRA,QTF,QTC,EN,NEW,CON,FLN(10)
        COMMON A(5000),INUM,IX,IY,KCYL,ELECT,SCALE,YSCALE
        COMMON /CCOM/ CONT(20),P(4),O(4)
        COMMON /PH/PHYS(8),IDEV
        DATA OLD,SAV,MOD,REF,TRA,QTF,QTC,EN,NEW,CON/'O','S','M','R',
     1 'T','Q','C','E','N','C'/
        CONOLD=0.0
        IPLOT=0
        CALL ASSIGN(3,'TT1:')
        CALL ASSIGN(5,'TI:')
        WRITE(5,52)
52      FORMAT(' SIZE(X,Y), IDEV ?')
        READ(5,54)PHYS(2),PHYS(4),IDEV
54      FORMAT(2F8.3,I1)
        PHYS(1)=0.0
        PHYS(3)=0.0
        PHYS(5)=0.0
        PHYS(6)=1023.0
        PHYS(7)=0.0
        PHYS(8)=780.0
50      WRITE(5,8)
8       FORMAT('$OPTION? ')
        READ(5,5)IO
5       FORMAT(A1)
        IF(IO.EQ.OLD) GO TO 100
        IF(IO.EQ.SAV) GO TO 200
        IF(IO.EQ.MOD) GO TO 300
        IF(IO.EQ.REF) GO TO 400
        IF(IO.EQ.TRA) GO TO 500
        IF(IO.EQ.QTF) GO TO 600
        IF(IO.EQ.NEW) GO TO 700
        IF(IO.EQ.CON) GO TO 800
        IF(IO.EQ.QTC) GO TO 900
        IF(IO.EQ.EN ) STOP
        GO TO 50
```

```
C       READ IN OLD POTENTIAL ARRAY FILE FROM UNIT 2

100     WRITE(5,23)
23      FORMAT('$POTENTIAL ARRAY, INPUT FILNAM.EXT ')
        READ(5,232)FLN
232     FORMAT(10A1)
        FLN(10)=0
        OPEN(UNIT=2,NAME=FLN,TYPE='OLD',FORM='UNFORMATTED')
        READ(2,ERR=999,END=1000)(KCYL,ELECT,IX,IY)
        INUM=IX*IY
        READ(2,ERR=999,END=1000)(A(I),I=1,INUM)
        SCALE=1023.0/(IX-1)
        YSCALE=780.0/(IY-1)
        CLOSE(UNIT=2)
        WRITE(5,7)
7       FORMAT('$FOR X & Y SCALES EQUAL, TYPE E, OR TOTAL SCREEN, T ')
        READ(5,5) IO
        IF(IO.EQ.TRA) GO TO 50
        IF(YSCALE.LT.SCALE) GO TO 120
        YSCALE=SCALE
120     SCALE=YSCALE
        GO TO 50

C       WRITE PRESENT POTENTIAL ARRAY FILE ONTO UNIT 2

200     WRITE(5,26)
26      FORMAT('$POTENTIAL ARRAY, OUTPUT FILNAM.EXT ')
        READ(5,232)FLN
        FLN(10)=0
        OPEN(UNIT=2,NAME=FLN,FORM='UNFORMATTED')
        WRITE(2,ERR=998,END=1000)(KCYL,ELECT,IX,IY)
        WRITE(2,ERR=998,END=1000)(A(I),I=1,INUM)
        CLOSE(UNIT=2)
        GO TO 50

C       ENTER ARRAY MODIFICATION ROUTINE

300     CALL BILD(0)
        GO TO 50

C       ENTER POTENTIAL REFINING ROUTINE

400     CALL REFINE
        GO TO 50

C       TRAJECTORY PLOTTING ROUTINE

500     CALL TRAJCT(IPLOT)
        GO TO 50

600     CALL QTRAJF(IPLOT)
        GO TO 50

C       ROUTINE FOR SETTING UP A NEW POTENTIAL ARRAY

700     WRITE(5,6)
6       FORMAT('$PLANAR GEOMETRY,TYPE -1,CYLINDRICAL SYMMETRY
        1, 0,PLANAR SYMMETRIC +1 ? ')
        READ(5,2,ERR=700)KCYL
705     WRITE(5,24)
24      FORMAT('$MAX. ELECTRODE POTENTIAL ? ')
        READ(5,4,ERR=705)ELECT
        ELECT2=ELECT*2.
708     WRITE(5,1)
1       FORMAT('$ARRAY DIMENSIONS,IX,IY ? ')
        READ(5,2,ERR=708)IX,IY
        INUM=IX*IY
```

```
      IF(INUM.GT.5600) GO TO 708
2     FORMAT(2I10)
4     FORMAT(F10.2)
      DO 710 I=1,INUM
710   A(I)=0.0
      SCALE=1023.0/(IX-1)
      YSCALE=780.0/(IY-1)
      WRITE(5,7)
      READ(5,5) IO
      IF(IO.EQ.TRA) GO TO 300
      IF(YSCALE.LT.SCALE) GO TO 720
      YSCALE=SCALE
720   SCALE=YSCALE
      GO TO 300

C     CONTOUR PLOTTING ROUTINE

800   CALL CONTUR(CONOLD)
      IPLOT=-1
      GO TO 50

900   CALL QTRAC(IPLOT)
      GO TO 50
998   PAUSE  'WRITE ERROR'
      GO TO 50
999   PAUSE  'READ ERROR'
      GO TO 50
1000  PAUSE  'END OF FILE'
      GO TO 50
      END
```

```
C       SUBROUTINE BILD
C
C       THIS PROGRAM BUILDS OR MODIFIES A POTENTIAL ARRAY USING
C       PROGRAMABLE GEOMETRIC FUNCTIONS.
C       RECTANGLE: THE LOWER LEFT COORDS, THE X-LENGTH & THE Y-LENGTH
C       NEED TO BE SPECIFIED .
C       TRIANGLE: THE LOWER LEFT COORDS THE X-LENGTH & THE ANGLE
C       (ACUTE IN DEG.) WITH THE X-AXIS.
C       CIRCLE: THE COORDS OF THE CENTER & THE RADIUS
C       POINT: THE COORDS OF THE POINT.
C       FOR EACH FUNCTION THE POTENTIAL NEEDS TO BE SPECIFIED.
C       ELECTRODE POINTS ARE DISTINGUISHED BY THE PROGRAMS BY A
C       VALUE OF ELECT2 (TWICE THE MAX. ELECTRODE POTENTIAL) BEING
C       ADDED TO THEIR POTENTIAL. HENCE POTENTIALS LESS THAN
C       HALF ELECT2 ARE NON ELECTRODE POTENTIALS. SPECIFYING E OR N
C       NOMINATES THE POTENTIAL AS AN ELECTRODE OR NOT. QUITE COMPLEX
C       SHAPES CAN BE CONSTRUCTED USING A SERIES OF FUNCTIONS,
C       SUCESSIVE ENTRIES ADDING TO OR BLOCKING OUT PARTS OF
C       PREVIOUS ONES.
C       BLOCK CHANGE: ALLOWS ONLY THE POINTS AT A SPECIFIED POTENTIAL
C       WITHIN THE SPECIFIED RECTANGLE TO BE CHANGED TO A NEW VALUE.
C       THIS IS ESPECIALLY USEFUL FOR MODIFYING THE POTENTIALS OF
C       ELECTRODES IN AN EXISTING POTENTIAL ARRAY.
C
        SUBROUTINE BILD(JPLOT)
        COMMON A(5000),INUM,IX,IY,KCYL,ELECT,SCALE,YSCALE
        COMMON/BCOM/B(40,6),IB(40)
        COMMON /PI/PHYS(8),ID
        LOGICAL EL1,EL2,RE,TR,BC,C1,PO,EX,EL,BL,Q,HE,NE
        DOUBLE PRECISION FU,VO
        DATA RE,TR,BC,C1,PO,EX,EL,NE,BL,HE,FU,VO/'R','T','B'
       1 ,'C','P','X','E','N',' ','H','FUNCTION',' VOLTAGE'/
1       FORMAT(A1,1X,4F10.2)
2       FORMAT(2(A1,1X,F10.2))
3       FORMAT(' AVAILABLE FUNCTIONS',/
       1 ' RECTANGLE;   R,(LOWER LEFT COORDS)X,Y,XLENGTH,YLENGTH',/
       1 '                #,POTENTIAL',/
       1 '                WHERE #=E FOR ELECTRODE OR N FOR NON',//
       1 ' BLOCK CHANGE; B,(L/L COORDS)X,Y,XLENGTH,YLENGTH',/
       1 '                #,OLD POTENTIAL,#,NEW POTENTIAL',//
       1 ' TRIANGLE;    T,(L/L COORDS)X,Y,XLENGTH,ANGLE WRT X-AXIS',/
       1 '                #,POTENTIAL',//
       1 ' CIRCLE;      C,(CENTRE COORDS)X,Y,RADIUS',/
       1 '                #,POTENTIAL',//
       1 ' POINT;       P,(CCORDS OF POINT)X,Y',/
       1 '                #,POTENTIAL',//
       1 ' EXECUTE:     X')
4       FORMAT(1X,A3,' DATA NOT IN CORRECT FORM, PLEASE RETYPE;'
       1 ' FOR HELP TYPE H !!!',/)
5       FORMAT(' FUNCTION DATA PLEASE?',/)
7       FORMAT(' DATA BUFFER FULL--EXECUTION COMMENCED.',/
       1 ' FOR FURTHER DATA INPUT REENTER MODIFY ROUTINE!')
8       FORMAT(' POTENTIAL LARGER THAN MAX.,REENTER LAST LINE',/)
        ELECT2=ELECT*2.
        NUM=0
47      WRITE(5,5)
48      NUM=NUM+1
49      READ(5,1,ERR=56) Q,(B(NUM,I),I=1,4)
        IF(Q.NE.BC) GO TO 50
        IB(NUM)=6
        GO TO 60
50      IF(Q.NE.RE) GO TO 51
        IB(NUM)=5
        GO TO 60
51      IF(Q.NE.TR) GO TO 52
        IB(NUM)=4
        GO TO 60
```

```
52      IF(Q.NE.CI) GO TO 53
        IB(NUM)=3
        GO TO 60
53      IF(Q.NE.PO) GO TO 54
        IB(NUM)=2
        B(NUM,3)=1.0
        B(NUM,4)=1.0
        GO TO 60
54      IF(Q.NE.EX) GO TO 55
        IB(NUM)=1
        GO TO 70
55      IF(Q.NE.HE) GO TO 56
57      WRITE(5,3)
        WRITE(5,5)
        GO TO 49
56      WRITE(5,4) FU
        GO TO 49
60      READ(5,2,ERR=65) EL1,B(NUM,5),EL2,B(NUM,6)
        IF(ABS(B(NUM,5)).GE.ELECT.OR.ABS(B(NUM,6)).GE.ELECT) GO TO 64
        IF(IB(NUM).NE.6.OR.EL2.EQ.NE) GO TO 61
        IF(EL2.NE.EL) GO TO 63
        B(NUM,6)=B(NUM,6)+ELECT2
61      IF(EL1.EQ.NE) GO TO 62
        IF(EL1.NE.EL) GO TO 63
        B(NUM,5)=B(NUM,5)+ELECT2
62      IF(NUM.LT.40) GO TO 43
        WRITE(5,7)
        GO TO 70
63      IF(EL1.EQ.HE) GO TO 57
65      WRITE(5,4) VO
        GO TO 60
64      WRITE(5,8)
        GO TO 60
70      XP=SCALE*(IX-1)
        YP=YSCALE*(IY-1)
        CALL PLOTC(XP,YP,1,PHYS,ID,1,0,0)
        DO 160 J=1,IY
        KT=(J-1)*IX
        DO 210 I=1,IX
        K=KT+I
        POTL=ELECT
        DO 200 L=1,NUM
        GO TO (200,300,400,500,300,300),IB(L)

C       RECTANGLE, POINT & BLOCK CHANGE

300     IF(I.LT.B(L,1).OR.I.GT.(B(L,1)+B(L,3)-.5)) GO TO 200
        IF(J.LT.B(L,2).OR.J.GT.(B(L,2)+B(L,4)-.5)) GO TO 200
        IF(IB(L).EQ.6) GO TO 310
        POTL=B(L,5)
        GO TO 200
310     IF(A(K).EQ.B(L,5)) POTL=B(L,6)
        GO TO 200

C       CIRCLE

400     F=1.0
        IF(B(L,4).LT.ELECT) F=-1.0
        RAD=B(L,3)+F*0.5
        IF(RAD.LT.SQRT((I-B(L,1))**2+(J-B(L,2))**2)) GO TO 200
        POTL=B(L,5)
        GO TO 200

C       TRIANGLE

500     IF(I.LT.B(L,1).OR.I.GT.B(L,1)+B(L,3)-.5) GO TO 200
        RHETA=B(L,4)*3.14159/180.
        YL=(I-B(L,1))*SIN(RHETA)/COS(RHETA)
```

```
      IF(YL) 510,520,520
520   IF(J.LT.B(L,2).OR.J.GT.B(L,2)+YL) GO TO 200
      GO TO 530
510   IF(J.LT.B(L,2)+YL.OR.J.GT.B(L,2))GO TO 200
530   POTL=B(L,5)
      GO TO 200
200   CONTINUE

C     UPDATE POTENTIAL

      IF(POTL-ELECT)260,280,270
260   A(K)=POTL
      GO TO 210
270   A(K)=POTL
280   IF(A(K).LT.ELECT) GO TO 210

C     PLOT IF AN ELECTRODE POINT

      XP=SCALE*(I-1)
      YP=YSCALE*(J-1)
      CALL PLOTC(XP,YP,1,PHYS,ID,1,1,0)
210   CONTINUE
160   CONTINUE
      CALL PLOTC(XP,YP,1,PHYS,ID,1,-1,1)
1000  RETURN
      END
```

```
C               SUBROUTINE REFINE
C
C       THIS SUBROUTINE ITERATIVELY REFINES AN ARRAY A(5000) OF
C       POTENTIAL POINTS. ELECTRODE POINTS DEFINED BY A VALUE OF
C       ELECT2 BEING ADDED TO THEIR POTENTIAL ARE NOT ALTERED.
C       OVER-RELAXATION UP TO 0.4 WILL SPEED THE PROCESS IN THE
C       EARLY STAGES. BETWEEN 100 & 1000 ITERATIONS WILL BE REQUIRED
C       DEPENDING ON THE ACCURACY REQUIRED IN THE TRAJECTORIES.
C       AT THE END OF EACH ITERATION THE SUM OF THE CHANGES IN
C       POTENTIALS OF ALL THE POINTS ALTERED DURING THAT ITERATION IS
C       PRINTED, THIS SHOULD GO TO NEAR ZERO EVENTUALLY. IF THIS
C       VALUE IS LESS THAN THE LOWER LIMIT SPECIFIED OR IF THE NUMBER
C       OF ITERATIONS IS REACHED CONTROL RETURNS TO THE MAIN PROGRAM.
C
C
        SUBROUTINE REFINE
        COMMON A(5000),INUM,LX,LY,KCYL,ELECT,SCALE,YSCALE
10      WRITE(5,1)
1       FORMAT(' NO. OF ITERATIONS,OVER-RELAXATION FACTOR,LOWER LIMIT')
        READ(5,2,ERR=10) NIT,OV,TLIM
2       FORMAT(I10,F10.1,F10.2)
        ELECT2=ELECT+ELECT
        ASSIGN 510 TO JSYM
        JLIM=LX*(LY-1)+1
        DO 1000 N=1,NIT
        ASSIGN 400 TO JHI
        IF(KCYL) 101,102,103
C       PLANAR NON-SYM
101     ASSIGN 510 TO JLO
        PB=0.0
        D=0.5
        DAD=0.3333333
        GO TO 104
C       CYLINDRICAL SYM
102     ASSIGN 530 TO JLO
        ASSIGN 520 TO JSYM
        D=0.3333333
        DAD=0.16666666
        GO TO 104
C       PLANAR SYM
103     ASSIGN 505 TO JLO
        D=0.3333333
        DAD=0.25
104     DSB=D
        K=0
        TOT=0.0
        DO 900 J=1,JLIM,LX
        P=0.0
C       TOP BOUNDARY?
        IF(J.LT.JLIM) GO TO 200
        PT=0.0
        D=0.5
        DAD=0.3333333
        DSB=D
        ASSIGN 500 TO JHI
        ASSIGN 510 TO JSYM
200     ILIM=J-1+LX
        DO 800 I=J,ILIM
C       ELECTRODE POINT?
        IF(A(I).GE.ELECT) GO TO 700
C       RIGHT BOUNDARY?
        IF(I.EQ.ILIM) GO TO 300
        PS=A(I+1)
        IF(PS.GE.ELECT) PS=PS-ELECT2
        P=P+PS
        GO TO JHI
300     D=DSB
```

```
        GO TO JHI
400     PT=A(I+LX)
        IF(PT.GE.ELECT) PT=PT-ELECT2
        GO TO JLO
500     PB=A(I-LX)
        IF(PB.GE.ELECT) PB=PB-ELECT2
        GO TO JSYM
505     PB=PT
510     P=(P+PT+PB)*D
        GO TO 600
520     P=(P+PT+PB)*D+(PT-PB)*DIV
        GO TO 600
530     P=P*D+PT*0.6666666
600     P=P+OV*(P-A(I))
C       TOTAL CHANGE OF CURRENT ITERATION
        TOT=TOT+ABS(P-A(I))
        A(I)=P
        GO TO 800
700     P=A(I)-ELECT2
800     D=DAD
        ASSIGN 500 TO JLO
        K=K+1
        DIV=0.125/K
        D=0.3333333
        DAD=0.25
900     DSB=D
        WRITE(3,2) N,TOT,OV
        IF(TOT.LT.TLIND RETURN
1000    CONTINUE
        RETURN
        END
```

```
C               SUBROUTINE CONTUR
C
C       THIS SUBROUTINE ALLOWS EQUIPOTENTIAL CONTOUR MAPS OF THE
C       POTENTIAL ARRAY TO BE DRAWN. UP TO 20 CONTOUR INTERVALS CAN BE
C       USED. THESE POTENTIALS ARE ENTERED AT RUN TIME FROM THE
C       SMALLEST TO THE LARGEST S ARE STORED IN A COMEON BLOCK.
C       THEY CAN BE REUSED BY TYPING 0 (ZERO) FOR THE NUMBER OF DESIRED
C       INTERVALS. STRAIGHT LINE SEGMENTS ARE DRAWN BETWEEN WHERE THE
C       CONTOUR LINES INTERCEPT THE HORIZONTAL & VERTICAL LINES JOINING
C       THE ARRAY POINTS.
C
C
        SUBROUTINE CONTUR(CONOLD)
        COMMON A(5000),INUM,NX,NY,KCYL,ELECT,SCALE,YSCALE
        COMMON /CCOM/ CON(20),P(4),Q(4)
        COMMON /PH/PHYS(3),ID
        DIST(C,P1,P2)=(C-P1)/(P2-P1)
1       FORMAT('SHOW MANY CONTOURS? ZERO FOR OLD  ')
2       FORMAT(I10)
3       FORMAT(' CONTOUR POTENTIALS, LEAST TO LARGEST')
4       FORMAT('S?')
5       FORMAT(F10.2)
        ELECT2=ELECT+ELECT
        PHYS(6)=(NX-1)*SCALE
        PHYS(3)=(NY-1)*YSCALE
        CALL PLOTC(0.0,0.0,1,PHYS,ID,1,0,0)
10      WRITE(5,1)
        READ(5,2,ERR=10) NCON
        IF(NCON) 10,20,30
30      IF(NCON.LT.2.OR.NCON.GT.20) GO TO 10

C       NEW SET OF CONTOURS?

        WRITE(5,3)
33      WRITE(5,4)
        READ(5,5,ERR=33) CON(1)
        CONMIN=CON(1)
        CONMAX=CON(1)
        DO 40 I=2,NCON
35      WRITE(5,4)
        READ(5,5,ERR=35) CON(I)
        IF(CON(I).LT.CONMIN) GO TO 10
        IF(CON(I).LE.CONMAX) GO TO 10
40      CONMAX=CON(I)
        CONOLD=NCON
20      IF(CONOLD.LE.0) GO TO 10

C       MARK ELECTRODE POTENTIALS.

        DO 41 IY=1,NY
        KY=(IY-1)*NX
        DO 41 IX=1,NX
        KX=KY+IX
        IF(A(KX).LT.ELECT) GO TO 41
        XP=SCALE*(IX-1)
        YP=YSCALE*(IY-1)
        CALL PLOTC(XP,YP,1,PHYS,ID,1,1,0)
41      CONTINUE
        NCON=CONOLD
```

```
C       SCAN THRU ARRAY CONSIDERING EACH SQUARE.

        DO 1000 IY=2,NY
        LY=(IY-1)*NX
        DO 1000 IX=2,NX
        L=LY+IX
        PMAX=-1.0E37
        PMIN=1.0E37
        I=IX
        J=IY

C       FIND MAX. & MIN. POTENTIALS OF CURRENT SQUARE.

        DO 120 K=1,4
        P(K)=A(L)
        IF(P(K).GE.ELECT) P(K)=P(K)-ELECT2
        IF(P(K).GT.PMAX) PMAX=P(K)
        IF(P(K).GE.PMIN) GO TO 99
        KROT=K-1
        PMIN=P(K)
99      GO TO (100,102,104,120),K
109     L=L-NX
        GO TO 120
102     L=L-1
        GO TO 120
104     L=L+NX
120     CONTINUE
        IF(PMAX.LE.CON(1).OR.PMIN.GE.CON(NCON)) GO TO 1000
        MINCON=NCON
        MAXCON=1

C       FIND MAX. & MIN. CONTOURS INTERCEPTING SQUARE.

        DO 200 I=2,NCON
        J=NCON-I+1
        IF(PMIN.LT.CON(J))MINCON=J
        IF(PMAX.GT.CON(I))MAXCON=I
200     CONTINUE
        IF(MINCON.GT.MAXCON) GO TO 1000
        I1=MOD(KROT,4)+1
        I2=MOD(KROT+1,4)+1
        I3=MOD(KROT+2,4)+1
        I4=MOD(KROT+3,4)+1

C       CALCULATE INTERCEPTS OF EACH CONTOUR WITH THE SIDES OF SQUARE.

        DO 900 I=MINCON,MAXCON
        DO 350 L0=1,4
350     O(LO)=-1.0
        ASSIGN 710 TO KPLOT
        IF(P(I2).LT.CON(I)) GO TO 400
        O(I1)=DIST(CON(I),P(I1),P(I2))
        IF(P(I3).LT.CON(I)) GO TO 600
        GO TO 450
400     IF(P(I3).LT.CON(I)) GO TO 650
        O(I2)=DIST(CON(I),P(I2),P(I3))
450     IF(P(I4).LT.CON(I)) GO TO 500
        O(I4)=DIST(CON(I),P(I4),P(I1))
        GO TO 700
500     O(I3)=DIST(CON(I),P(I3),P(I4))
        GO TO 700
600     O(I2)=DIST(CON(I),P(I2),P(I3))
650     IF(P(I4).LT.CON(I)) GO TO 700
        O(I3)=DIST(CON(I),P(I3),P(I4))
        O(I4)=DIST(CON(I),P(I4),P(I1))
```

```
C       DRAW CONTOUR LINE SEGMENTS.

700     DO 800 J=1,4
        IF(O(J).EQ.-1.0) GO TO 800
        GO TO (701,702,703,704),J
701     XP=SCALE*(IX-1)
        YP=YSCALE*(IY-1-O(1))
        GO TO KPLOT
702     XP=SCALE*(IX-1-O(2))
        YP=YSCALE*(IY-2)
        GO TO KPLOT
703     XP=SCALE*(IX-2)
        YP=YSCALE*(IY-2+O(3))
        GO TO KPLOT
704     XP=SCALE*(IX-2+O(4))
        YP=YSCALE*(IY-1)
        GO TO KPLOT
710     CALL PLOTC(XP,YP,1,PHYS,ID,1,1,-1)
        ASSIGN 720 TO KPLOT
        GO TO 800
720     CALL PLOTC(XP,YP,1,PHYS,ID,1,1,1)
        ASSIGN 710 TO KPLOT
800     CONTINUE
900     CONTINUE
1000    CONTINUE
        CALL PLOTC(XP,YP,1,PHYS,ID,1,-1,0)
        RETURN
        END
```

```
C              PROGRAM TRAJCT
C
C     THIS SUBROUTINE CALCS. & PLOTS THE TRAJECTORIES OF IONS OR
C     ELECTRONS IN REAL TIME & SPACE. ENERGIES ARE IN ELECTRON
C     VOLTS ,DIMENSIONS IN MILLIMETERS. ALL VOLTAGES CAN BE
C     SCALED UP OR DOWN USING THE VSCALE PARAMETER & THE TIME
C     INTERVAL BETWEEN SUCESSIVE FORCE CALCS. ADJUSTED WITH THE TIME
C     INT. M/E, THE MASS/CHARGE RATIO OF THE ION & THE ACTUAL GRID
C     SPACING IN MILLIMETERS NEED TO BE SPECIFIED. THE OTHER VARIABLES
C     ARE THE STARTING COORDS, THE INITIAL ENERGY & THE INITIAL
C     ANGLE. ANY OR ALL OF THESE VALUES CAN BE INCREMENTED BY A
C     CONSTANT AMOUNT FOR EACH SUCESSIVE TRAJECTORY.
C     THE TRAJECTORY IS PLOTTED AS A SERIES OF STRAIGHT LINE SEGMENTS
C     DRAWN EACH TIME THE ION MOVES INTO A NEW SQUARE. STARTING &
C     FINISHING COORDS AND ENERGIES, THE POSITIONS OF ANY
C     CROSSOVERS OF THE X AXIS AND THE TOTAL ACCUMULATED ERROR
C     ARE RECORDED.
C     ION FRAGMENTATIONS TO A SPECIFIED NEW MASS CAN BE CARRIED OUT
C     AT A SPECIFIED X VALUE.
C     THE ELECTROSTATIC FORCE ON THE ION IS CALCULATED FROM A LINEAR
C     INTERPOLATION BETWEEN ELECTRODE POINTS, HOWEVER TO IMPROVE
C     THE FIT A QUADRATIC INTERPOLATION IS USED NEAR AN AXIS
C     OF SYMMETRY(X-AXIS).
C
C
      SUBROUTINE TRAJCT(IPLOT)
      COMMON A(5000),INUM,NX,NY,KCYL,ELECT,SCALE,YSCALE
      COMMON/CCOM/CON(20),P(8)
      COMMON /PH/PHYS(8),ID
      LOGICAL PLOT,JPLOT
      DATA PLOT/'N'/
      ELECT2=ELECT*2.
67    WRITE(5,5)
      READ(5,6,ERR=67) DM,VSCALE,T
66    WRITE(5,8)
      READ(5,6,ERR=66) EM,EM2,DEM
6     FORMAT(5F10.2)
      IF(T.EQ.0.0)T=1.0
      IF(EM.EQ.0.0) EM=1.0
      IF(DM.EQ.0.0) DM=1.0
      IF(VSCALE.EQ.0.0) VSCALE=1.0
      IF(EM2.EQ.0.0)GO TO 65
64    WRITE(5,11)
      READ(5,6,ERR=64)XDISOC,DXD
      GO TO 63
65    EM2=EM
63    T1=SQRT(ABS(EM))/(T*10000.)
      T2=T1/2.0
      DM=DM*DM*1.03649E-2
      EM=EM*DM
      EM2=EM2*DM
      FEM=VSCALE*T1/EM
      FEM2=VSCALE*T1/EM2
68    WRITE(5,1)
      READ (5,2,ERR=68) X,Y,DX,DY
69    WRITE(5,3)
      READ (5,2,ERR=69) ES,THETA,DE,DTHET
1     FORMAT('0STARTING COORDS X,Y,INCREMENTS DX,DY ')
2     FORMAT(4F10.2)
3     FORMAT('0ION ENERGY,ANGLE WRT X AXIS(DEG),INCRS DE,DTHET  ')
5     FORMAT('0GRID SPACING(MM),VOLTAGE SCALING,TIME INT. ')
8     FORMAT('0M/E OF ION,M/E OF FRAGMENT  ')
11    FORMAT('0X-COORD OF DISSOCIATION, X-INCREMENT  ')
12    FORMAT('0HOW MANY TRAJECTORIES,FOR NEW PLOT TYPE N  ')
70    WRITE(5,12)
      READ (5,4,ERR=70) NTRAJ,JPLOT
4     FORMAT(I10,A1)
      IF(JPLOT.NE.PLOT.AND.IPLOT.NE.0) GO TO 400
      IPLOT=1
```

```
C       NEW PLOT-CLEAR SCREEN & MARK ELECTRODES

410     XP=SCALE*(NX-1)
        YP=YSCALE*(NY-1)
        CALL PLOTC(0.0,0.0,1,PHYS,ID,1,0,-1)
        DO 701 J=1,NY-2
        K=J*NX+1
        DO 701 I=1,NX-2
        K=K+1
        Q=A(K)
        IF(Q.LT.ELECT) GO TO 701
        IF(Q.EQ.A(K-NX).AND.Q.EQ.A(K+NX).AND.Q.EQ.A(K-1).AND.Q.EQ.
       1   A(K+1)) GO TO 701
        XP=SCALE*I
        YP=YSCALE*J
        CALL PLOTC(XP,YP,1,PHYS,ID,1,1,0)
701     CONTINUE
400     CONTINUE
        DO 200 NT=1,NTRAJ
        ASSIGN 14 TO IPOTL
        X0=X+(NT-1)*DX
        Y0=Y+(NT-1)*DY

C       CALC INITIAL X&Y VELOCITIES

        V=SQRT(ABS(2.0*ES/EMD))
        ES=ES+DE
        THET=THETA+(NT-1)*DTHET
        THETI=THET*3.14159/180.
        DISOC=XDISOC+(NT-1)*DXD
        VX0=V*COS(THETI)
        VY0=V*SIN(THETI)
304     SEN=0.5*V*V*EM
        WRITE(5,7) X0,Y0,SEN,THET
7       FORMAT(' INITIAL X=',F6.2,' Y=',F6.2,' ENERGY=',F8.2,' ANGLE='
       1 ,F7.2)
        XP=SCALE*(X0-1)
        YP=YSCALE*(Y0-1)
        CALL PLOTC(XP,YP,1,PHYS,ID,1,1,-1)
307     IOX=0
        IOY=0
        ELOSS=0.0
        FM=FEM
        EMASS=EM
        DO 10 NITER=1,25000
        IF(EMASS.EQ.EM2.OR.X0.LT.DISOC) GO TO 195
        FM=FEM2
        EMASS=EM2
        ELOSS=0.5*(VX0*VX0+VY0*VY0)*(EM-EM2)
        WRITE(5,13) X0,Y0,ELOSS
13      FORMAT(' DISSOCIATION AT X=',F6.2,' Y=',F6.2,' ENERGY LOSS=',
       1  F8.2)
195     IX=X0
        IF(Y0-1.)197,198,198

C       CROSSING OF X-AXIS?

197     IF(XCYL.LT.0) GO TO 9
        Y0=2.0-Y0
        VY0=-VY0
        WRITE(5,196)X0
196     FORMAT(' CROSSOVER AT X=',F6.2)
198     IY=Y0

C       NEW POTENTIAL SURFACE CALC. REQUIRED?

17      IF(IX.EQ.IOX.AND.IY.EQ.IOY) GO TO 130
```

```
C       ION HAS MOVED TO NEW SQUARE- UPDATE TRAJECTORY PLOT

        XP=SCALE*(X0-1)
        YP=YSCALE*(Y0-1)
        IXP=XP
        IYP=YP
        IF(IXP.LT.0.OR.IXP.GT.1023.OR.IYP.LT.0.OR.IYP.GT.780)GO TO 57
        CALL PLOTC(XP,YP,1,PHYS,ID,1,1,1)
57      IX1=IX+1
        IY1=IY+1
        IF(IX1.GT.NX.OR.IY1.GT.NY.OR.IX.LT.1) GO TO 9
        NIM=0
        NOM=0
93      IOY=IY
97      IOX=IX

C       FIND POTENTIALS OF 4 POINTS SURROUNDING ION

        DO 100 J=IY,IY1
        DO 100 I=IX,IX1
        K=I+(J-1)*NX
        NIM=NIM+1
        P(NIM)=A(K)

C       IF POINT IS AN ELECTRODE POINT SUBTRACT ELECT2 FROM POTENTIAL.

        IF(P(NIM)-ELECT) 100,99,99
99      P(NIM)=P(NIM)-ELECT2
        NOM=NOM+1
        IF(NOM.EQ.3) ASSIGN 9 TO IPOTL

C       HITS ELECTRODE

100     CONTINUE
130     DSX=X0-IX
        DSY=Y0-IY
        P(5)=P(1)+DSX*(P(2)-P(1))
        P(6)=P(3)+DSX*(P(4)-P(3))
        P(7)=P(1)+DSY*(P(3)-P(1))
        P(8)=P(2)+DSY*(P(4)-P(2))

C       CALC POTENTIAL GRADIENTS >FORCES >NEW VELOCITIES >NEW POSITION

        FX=P(7)-P(8)
        FY=P(5)-P(6)
        IF(Y0.LT.2.0.AND.KCYL.GE.0) FY=(FY+FY)*(Y0-1.)
23      VXN=VX0+FX*FM
        VYN=VY0+FY*FM
610     X0=X0+(VX0+VXN)*T2
        Y0=Y0+(VY0+VYN)*T2
        VY0=VYN
        VX0=VXN
        GO TO IPOTL
14      ASSIGN 10 TO IPOTL

C       CALC POTENTIAL AT STARTING COORDS

        STAPOT=VSCALE*(P(5)+DSY*(P(6)-P(5)))
10      CONTINUE

C       DRAW FINAL SEGMENT OF TRAJECTORY

9       IXP=SCALE*(X0-1)
        IYP=YSCALE*(Y0-1)
        IF(IXP.LT.0.OR.IXP.GT.1023.OR.IYP.LT.0.OR.IYP.GT.780)GO TO 601
        XP=IXP
        YP=IYP
        CALL PLOTC(XP,YP,1,PHYS,ID,1,1,1)
```

```
C       CALC POTENTIAL AT FINAL COORDS

601     POTL=VSCALE*(P(5)+DSY*(P(6)-P(5)))
        ENERGY=0.5*(VX0*VX0+VY0*VY0)*EMASS
        ANGLE=ATAN(VY0/VX0)
        ANGLE=ANGLE*180./3.14159
        IF(VY0.LT.0.0) ANGLE=ANGLE-180.

C       CALC ERROR BY CONSERVATION OF ENERGY

        ERROR=ABS(POTL-STAPOT)-ABS(SEN-ENERGY-ELOSS)
        TOF=NITER*TI
431     WRITE(5,219)X0,Y0,ENERGY,ANGLE
219     FORMAT('   FINAL  X=',F6.2,' Y=',F6.2,' ENERGY=',F8.2,' ANGLE='
        1 ,F7.2)
        WRITE(5,218)ERROR,TOF
218     FORMAT(' ERROR=',F8.2,'  TIME OF FLIGHT=',F8.3,' MICROSECS.')
200     CONTINUE
        CALL PLOTC(XP,YP,1,PHYS,ID,1,-1,-1)
        RETURN
        END
```

```
C     SUBROUTINE QTRAJF
C
C          THIS SUBROUTINE CALCULATES & PLOTS THE TRAJECTORIES
C     OF IONS OR ELECTRONS IN REAL TIME & SPACE.  ENERGIES ARE
C     IN ELECTRON VOLTS, DIMENTIONS IN MILLIMETERS.  ALL VOLTAGES
C     CAN BE SCALED UP OR DOWN USING THE VSCALE PARAMETER & THE
C     TIME INTERVAL BETWEEN SUCCESSIVE FORCE CALCULATIONS ADJUSTED
C     WITH THE TIME INTERVAL.  M/Z, THE MASS/CHARGE RATIO OF THE
C     IONS, AND THE ACTUAL GRID SPACING IN MILLIMETERS NEED TO BE
C     SPECIFIED.  THE OTHER VARIABLES ARE THE STARTING COORDINATES,
C     THE INITIAL ENERGY & THE INITIAL ANGLE.  ANY OR ALL OF THESE
C     VALUES CAN BE INCREMENTED BY A CONSTANT AMOUNT FOR EACH
C     SUCCESSIVE TRAJECTORY.
C          THE TRAJECTORY IS PLOTTED AS A SERIES OF STRAIGHT
C     LINE SEGMENTS DRAWN EACH TIME THE ION MOVES INTO A NEW
C     SQUARE.  STARTING & FINISHING COORDINATES, AND ENERGIES,
C     THE POSITIONS OF ANY CROSSOVERS OF THE X-AXIS AND THE
C     TOTAL ACCUMULATED ERROR ARE RECORDED.
C          ION FRAGMENTATIONS TO A SPECIFIED NEW MASS CAN BE
C     CARRIED OUT AT A SPECIFIED X VALUE.
C          THE ELECTROSTATIC FORCE ON THE ION IS CALCULATED
C     FROM A LINEAR INTERPOLATION BETWEEN ELECTRODE POINTS,
C     HOWEVER TO IMPROVE THE FIT A QUADRATIC INTERPOLATION IS
C     USED NEAR AN AXIS OF SYMMETRY (X-AXIS).
C
C
      SUBROUTINE QTRAJF(IPLOT)
      DIMENSION FAC(100)
      COMMON A(5000),INUM,NX,NY,KCYL,ELECT,SCALE,YSCALE
      COMMON /CCOM/ CON(20),P(8)
      COMMON /PHY/ PHYS(8),ID
      LOGICAL NPLOT,JPLOT
      DATA NPLOT/'N'/
      CALL ASSIGN(2,'QTABLE.BIN')
      READ(2)(FAC(I),I=1,100)
      CALL CLOSE (2)
      ELECT2=ELECT*2.0
      WRITE(5,1)
1     FORMAT('0SUBROUTINE QTRF')
10    WRITE(5,11)
11    FORMAT('0GRID SPACING(MM), VOLTAGE SCALING, FREQUENCY, A/Q ')
      READ(5,12,ERR=10) DM,VSCALE,FREQ,RFDC
12    FORMAT(5F10.2)
14    DO 15 I=1,100
      FAC(I)=FAC(I)+RFDC
15    CONTINUE
20    WRITE(5,21)
21    FORMAT('$M/Z OF ION, M/Z OF FRAGMENT, DI, DF ')
      READ(5,12,ERR=20) CEM,CEM2,DEM,DEM2
      IF(FREQ.EQ.0.0) FREQ=2.0
      IF(CEM.EQ.0.0)    CEM=1.0
      IF(DM.EQ.0.0)      DM=1.0
      IF(VSCALE.EQ.0.0) VSCALE=1.0
      IF(CEM2.EQ.0.0)    GOTO 40
30    WRITE(5,31)
31    FORMAT('$TIME OF DISSOCIATION, TIME INCREMENT ')
      READ(5,12,ERR=30) TDISOC,DTD
      GOTO 50
40    CEM2=CEM
50    T1=0.01/FREQ
      T2=T1/2.0
      DM=DM*DM*1.03649E-2
60    WRITE(5,61)
61    FORMAT('$STARTING COORDS X,Y, INCREMENTS DX, DY ')
      READ(5,12,ERR=60) X,Y,DX,DY
      WRITE(5,71)
71    FORMAT(' ION ENERGY, ANGLE WRT X-AXIS (DEG), INCRS DE,DTHET ')
      READ(5,12,ERR=70) ES,THETA,DE,DTHET
```

```
74      WRITE(5,75)
75      FORMAT(' AXIAL ENERGY, QUAD LENGTH, ORIFICE, NCYCL ')
        READ(5,76,ERR=70) EA,QL,ORF,NCY
76      FORMAT(3F10.2,I5)
80      WRITE(5,81)
81      FORMAT('$HOW MANY TRAJECTORIES?  FOR NEW PLOT TYPE N ')
        READ(5,82,ERR=80) NTRAJ,JPLOT
82      FORMAT(I10,A1)
84      FORMAT(I8,21X,A1)
        IF(JPLOT.NE.NPLOT.AND.IPLOT.NE.0) GOTO 170
        IPLOT=1
C
C       NEW PLOT -- CLEAR SCREEN & MARK ELECTRODES.
100     PHYS(6)=SCALE*(NX-1)
        PHYS(8)=YSCALE*(NY-1)
110     CALL PLOTC(0.0,0.0,1,PHYS,ID,1,0,1)
120     DO 160 J=1,NY-2
        K=J*NX+1
130     DO 150 I=1,NX-2
        K=K+1
        Q=A(K)
        IF(Q.LT.ELECT) GOTO 150
        IF(Q.EQ.A(K-NX).AND.Q.EQ.A(K+NX).AND.Q.EQ.A(K-1).AND.
     1  Q.EQ.A(K+1)) GOTO 150
        XP=SCALE*I
        YP=YSCALE*J
140     CALL PLOTC(XP,YP,1,PHYS,ID,1,1,0)
150     CONTINUE
160     CONTINUE
170     DO 1400 NT=1,NTRAJ
        ASSIGN 920 TO IPOTL
        EM=(CEM*(NT-1)*DEM)*DM
        EM2=(CEM2+(NT-1)*DEM2)*DM
        FEM=VSCALE*T1/EM
        FEM2=VSCALE*T1/EM2
        TRP=QL*SQRT(ABS(CEM*0.51822/EA))
        X0=X+(NT-1)*DX
        Y0=Y+(NT-1)*DY
C
C       CALCULATE INITIAL X & Y VELOCITIES.
200     V=SQRT(ABS(2.0*ES/EM))
        ES=ES+DE
        THET=THETA+(NT-1)*DTHET
        THETI=THET*3.1415926/180.0
204     DISOC=TDISOC+(NT-1)*DTD
        VX0=V*COS(THETI)
        VY0=V*SIN(THETI)
210     SEN=0.5*V*V*EM
        WRITE(5,212) X0,Y0,SEN,THET
212     FORMAT('0INITIAL X=',F8.2,4X,'Y=',F8.2,4X,'ENERGY=',F10.2,
     14X,'ANGLE=',F8.2)
        XP=SCALE*(X0-1.0)
        YP=YSCALE*(Y0-1.0)
215     CALL PLOTC(XP,YP,1,PHYS,ID,1,1,-1)
220     IOX=0
        IOY=0
        ELOSS=0.0
        FM=FEM
        EMASS=EM
        TOF=-TI
        IF(NCY.EQ.0) NCY=250
221     DO 1000 NITER=1,NCY
222     DO 950 IFR=1,100
        TOF=TOF+TI
240     IF(EMASS.EQ.EM2.OR.TOF.LT.DISOC) GOTO 280
        FM=FEM2
        EMASS=EM2
        ELOSS=0.5*(VX0*VX0 + VY0*VY0) * (EM-EM2)
```

```
      WRITE(5,275) X0,Y0,ELOSS
275   FORMAT(' DISSOCIATION AT X=',F8.2,4X,'Y=',F8.2,4X,'ENERGY
     1 LOSS=',F10.2)
290     IX=X0
        IF(Y0-1.0)300,310,310
C
C     CROSSING OF X-AXIS?
300   IF(KCYL.LT.0) GOTO 1100
        Y0=2.0-Y0
        VY0=-VY0
        WRITE(5,301) X0
301   FORMAT(' CROSSOVER AT X=',F8.2)
310   IY=Y0
C
C     NEW POTENTIAL SURFACE CALCULATION REQUIRED ?
400   IF(IX.EQ.IOX.AND.IY.EQ.IOY) GOTO 360
C
C     ION HAS MOVED TO NEW SQUARE. -- UPDATE TRAJECTORY PLOT.
        IXP=SCALE*(X0-1.0)
        IYP=YSCALE*(Y0-1.0)
        IF(IXP.LT.0.OR.IXP.GT.1023.OR.IYP.LT.0.OR.IYP.GT.780) GOTO 500
        XP=IXP
        YP=IYP
450   CALL PLOTC(XP,YP,1,PHYS,ID,1,1,1)
500     IX1=IX+1
        IY1=IY+1
        IF(IX1.GT.NX.OR.IY1.GT.NY.OR.IX.LT.1) GOTO 1100
        NIM=0
        NOM=0
510     IOY=IY
520     IOX=IX
C
C     FIND POTENTIALS OF 4 POINTS SURROUNDING ION.
600   DO 850 J=IY,IY1
610   DO 800 I=IX,IX1
        K=I+(J-1)*NX
        NIM=NIM+1
        P(NIM)=A(K)
C
C     IF POINT IS AN ELECTRODE POINT, SUBTRACT ELECT2 FROM POTENTIAL.
700   IF(P(NIM)-ELECT) 800,710,710
710   P(NIM)=P(NIM)-ELECT2
        NOM=NOM+1
        IF(NOM.EQ.3) ASSIGN 1100 TO IPOTL
C
C     HITS ELECTRODE.
800   CONTINUE
850   CONTINUE
860   DSX=X0-IX
        DSY=Y0-IY
        P(5)=P(1)+DSX*(P(2)-P(1))
        P(6)=P(3)+DSX*(P(4)-P(3))
        P(7)=P(1)+DSY*(P(3)-P(1))
        P(8)=P(2)+DSY*(P(4)-P(2))
C
C     CALC POTENTIAL GRADIENTS >FORCES >NEW VELOCITIES >NEW POSITION.
900   FX=P(7)-P(8)
        FY=P(5)-P(6)
        IF(Y0.LT.2.0.AND.KCYL.GE.0) FY=(FY+FY)*(Y0-1.0)
905   VXN=VX0 + FX*FN*FAC(IFR)
        VYN=VY0 + FY*FN*FAC(IFR)
910   X0 = X0 + (VX0+VXN)*T2
        Y0 = Y0 + (VY0+VYN)*T2
        VY0=VYN
        VX0=VXN
        GOTO IPOTL
920   ASSIGN 950 TO IPOTL
```

```
C
C     CALCULATE POTENTIAL AT STARTING COORDINATES.
930   STAPOT=VSCALE*(P(5)+DSY*(P(6)-P(5)))*FAC(IFR)
950   CONTINUE
1000  CONTINUE
      IFR=1
C
C     DRAW FINAL SEGMENT OF TRAJECTORY.
1100  IXP=SCALE*(X0-1.0)
      IYP=YSCALE*(Y0-1.0)
      IF(IXP.LT.0.OR.IXP.GT.1023.OR.IYP.LT.0.OR.IYP.GT.783) GOTO 1200
      XP=IXP
      YP=IYP
1150  CALL PLOTC(XP,YP,1,PHYS,ID,1,1,1)
C
C     CALCULATE POTENTIAL AT FINAL COORDINATES.
1200  POTL=VSCALE*FAC(IFR)*(P(5)+DSY*(P(6)-P(5)))
      DST=GS*SQRT(ABS((X0-35.5)**2+(Y0-35.5)**2))
      ENERGY=0.5*(VX0*VX0+VY0*VY0)*EMASS
      ANGLE =ATAN(VY0/VX0)
      ANGLE =ANGLE*180.0/3.1415926
      IF(VY0.LT.0.0) ANGLE=ANGLE-180.0
C
C     CALCULATE ERROR BY CONSERVATION OF ENERGY.
1300  ERROR=ABS(POTL-STAPOT)-ABS(SEN-ENERGY-ELOSS)
      IF(TOF.GT.TNP) GO TO 1305
      WRITE(5,*)'UNSTABLE'
      GO TO 1310
1305  IF(ORF.GT.DST) GO TO 1306
      WRITE(5,*)'STABLE'
      GO TO 1310
1306  WRITE(5,*)'PASS'
1310  WRITE(5,1311) X0,Y0,ENERGY,ANGLE
1311  FORMAT(' FINAL    X=',F8.2,4X,'Y=',F8.2,4X,'ENERGY=',F10.2,
     14X,'ANGLE=',F8.2)
      WRITE(5,1312) ERROR,TNP,TOF
1312  FORMAT('  ERROR=',F10.2,4X,'TNP=',F10.4,4X,'TOF=',F10.4,
     1' MICROSECONDS.')
1400  CONTINUE
1450  CALL PLOTC(XP,YP,1,PHYS,ID,1,-1,0)
1500  RETURN
      END
```

```
C     SUBROUTINE QTRAG
C
C          THIS SUBROUTINE CALCULATES & PLOTS THE TRAJECTORIES
C     OF IONS OR ELECTRONS IN REAL TIME & SPACE.  ENERGIES ARE
C     IN ELECTRON VOLTS, DIMENTIONS IN MILLIMETERS.  ALL VOLTAGES
C     CAN BE SCALED UP OR DOWN USING THE VSCALE PARAMETER & THE
C     TIME INTERVAL BETWEEN SUCCESSIVE FORCE CALCULATIONS ADJUSTED
C     WITH THE TIME INTERVAL.  M/Z, THE MASS/CHARGE RATIO OF THE
C     IONS, AND THE ACTUAL GRID SPACING IN MILLIMETERS NEED TO BE
C     SPECIFIED.  THE OTHER VARIABLES ARE THE STARTING COORDINATES,
C     THE INITIAL ENERGY & THE INITIAL ANGLE.  ANY OR ALL OF THESE
C     VALUES CAN BE INCREMENTED BY A CONSTANT AMOUNT FOR EACH
C     SUCCESSIVE TRAJECTORY.
C          THE TRAJECTORY IS PLOTTED AS A SERIES OF STRAIGHT
C     LINE SEGMENTS DRAWN EACH TIME THE ION MOVES INTO A NEW
C     SQUARE.  STARTING & FINISHING COORDINATES, AND ENERGIES,
C     THE POSITIONS OF ANY CROSSOVERS OF THE X-AXIS AND THE
C     TOTAL ACCUMULATED ERROR ARE RECORDED.
C          ION FRAGMENTATIONS TO A SPECIFIED NEW MASS CAN BE
C     CARRIED OUT AT A SPECIFIED X VALUE.
C          THE ELECTROSTATIC FORCE ON THE ION IS CALCULATED
C     FROM A LINEAR INTERPOLATION BETWEEN ELECTRODE POINTS,
C     HOWEVER TO IMPROVE THE FIT A QUADRATIC INTERPOLATION IS
C     USED NEAR AN AXIS OF SYMMETRY (X-AXIS).
C
C
      SUBROUTINE QTRAG(IPLOT)
      DIMENSION FAC(100)
      COMMON A(5000),INUM,NX,NY,KCYL,ELECT,SCALE,YSCALE
      COMMON /CCOM/ CON(20),P(8)
      COMMON /PH/ PHYS(8),ID
      LOGICAL NPLOT,JPLOT
      DATA NPLOT/'N'/
      CALL ASSIGN(2,'QTABLE.BIN')
      READ(2)(FAC(I),I=1,100)
      CALL CLOSE (2)
      ELECT2=ELECT*2.0
      WRITE(5,1)
1     FORMAT('0SUBROUTINE QTRF')
10    WRITE(5,11)
11    FORMAT('0GRID SPACING(MM), VOLTAGE SCALING, FREQUENCY, A/Q ')
      READ(5,12,ERR=10) DM,VSCALE,FREQ,RFDC
12    FORMAT(5F10.2)
14    DO 15 I=1,100
      FAC(I)=FAC(I)+RFDC
15    CONTINUE
20    WRITE(5,21)
21    FORMAT('$M/Z OF ION, M/Z OF FRAGMENT, DI, DF ')
      READ(5,12,ERR=20) CEM,CEM2,DEM,DEM2
      IF(FREQ.EQ.0.0) FREQ=2.0
      IF(CEM.EQ.0.0)    CEM=1.0
      IF(DM.EQ.0.0)      DM=1.0
      IF(VSCALE.EQ.0.0) VSCALE=1.0
      IF(CEM2.EQ.0.0)   GOTO 40
30    WRITE(5,31)
31    FORMAT('$X-COORD OF DISSOCIATION, X INCREMENT ')
      READ(5,12,ERR=30) XDISOC,DXD
      GOTO 50
40    CEM2=CEM
50    T1=0.01/FREQ
      T2=T1/2.0
      DM=DM*DM*1.03649E-2
60    WRITE(5,61)
61    FORMAT('$STARTING COORDS X,Y, INCREMENTS DX, DY ')
      READ(5,12,ERR=60) X,Y,DX,DY
70    WRITE(5,71)
71    FORMAT(' ION ENERGY, ANGLE WRT X-AXIS (DEG), INCRS DE,DTHET ')
      READ(5,12,ERR=70) ES,THETA,DE,DTHET
```

```
74      WRITE(5,75)
75      FORMAT(' AXIAL ENERGY, QUAD LENGTH, ORIFICE, NCYCL ')
        READ(5,76,ERR=70) EA,QL,ORF,NCY
76      FORMAT(3F10.2,I5)
80      WRITE(5,81)
81      FORMAT('SHOW MANY TRAJECTORIES?  FOR NEW PLOT TYPE N ')
        READ(5,82,ERR=80) NTRAJ,JPLOT
82      FORMAT(I10,A1)
84      FORMAT(18,21X,A1)
        IF(JPLOT.NE.NPLOT.AND.IPLOT.NE.0) GOTO 170
        IPLOT=1
C
C       NEW PLOT -- CLEAR SCREEN & MARK ELECTRODES.
100     PHYS(6)=SCALE*(NX-1)
        PHYS(8)=YSCALE*(NY-1)
110     CALL PLOTC(0.0,0.0,1,PHYS,ID,1,0,1)
120     DO 160 J=1,NY-2
        K=J*NX+1
130     DO 150 I=1,NX-2
        K=K+1
        Q=A(K)
        IF(Q.LT.ELECT) GOTO 150
        IF(Q.EQ.A(K-NX).AND.Q.EQ.A(K+NX).AND.Q.EQ.A(K-1).AND.
     1  Q.EQ.A(K+1)) GOTO 150
        XP=SCALE*I
        YP=YSCALE*J
140     CALL PLOTC(XP,YP,1,PHYS,ID,1,1,0)
150     CONTINUE
160     CONTINUE
170     DO 1400 NT=1,NTRAJ
        ASSIGN 920 TO IPOTL
        EM=(CEM+(NT-1)*DEMD)*DM
        EM2=(CEM2+(NT-1)*DEM2)*DM
        FEM=VSCALE*TI/EM
        FEM2=VSCALE*TI/EM2
        TNP=QL*SQRT(ABS(CEM*0.51822/EA))
        X0=X+(NT-1)*DX
        Y0=Y+(NT-1)*DY
C
C       CALCULATE INITIAL X & Y VELOCITIES.
200     V=SQRT(ABS(2.0*ES/EMD))
        ES=ES+DE
        THET=THETA+(NT-1)*DTHET
        THETI=THET*3.1415926/180.0
204     DISOC=XD(ISOC+(NT-1)*DXD
        VX0=V*COS(THETI)
        VY0=V*SIN(THETI)
210     SEN=0.5*V*V*EM
        WRITE(5,212) X0,Y0,SEN,THET
212     FORMAT('0INITIAL X=',F8.2,4X,'Y=',F8.2,4X,'ENERGY=',F10.2,
     14X,'ANGLE=',F8.2)
        XP=SCALE*(X0-1.0)
        YP=YSCALE*(Y0-1.0)
215     CALL PLOTC(XP,YP,1,PHYS,ID,1,1,-1)
220     IOX=0
        IOY=0
        ELOSS=0.0
        FM=FEM
        EMASS=EM
        TOF=-TI
        IF(NCY.EQ.0) NCY=250
221     DO 1000 NITER=1,NCY
222     DO 950 IFR=1,100
        TOF=TOF+TI
240     IF(EMASS.EQ.EM2.OR.X0.LT.DISOC) GOTO 280
        FM=FEM2
        EMASS=EM2
        ELOSS=0.5*(VX0*VX0 + VY0*VY0) * (EM-EM2)
```

```
      WRITE(5,275) X0,Y0,ELOSS
275   FORMAT(' DISSOCIATION AT X=',F8.2,4X,'Y=',F8.2,4X,'ENERGY
     1 LOSS=',F10.2)
280   IX=X0
      IF(Y0-1.0)300,310,310
C
C     CROSSING OF X-AXIS?
300   IF(KCYL.LT.0) GOTO 1100
      Y0=2.0-Y0
      VY0=-VY0
      WRITE(5,301) X0
301   FORMAT(' CROSSOVER AT X=',F8.2)
310   IY=Y0
C
C     NEW POTENTIAL SURFACE CALCULATION REQUIRED ?
400   IF(IX.EQ.IOX.AND.IY.EQ.IOY) GOTO 860
C
C     ION HAS MOVED TO NEW SQUARE. -- UPDATE TRAJECTORY PLOT.
      IXP=SCALE*(X0-1.0)
      IYP=YSCALE*(Y0-1.0)
      IF(IXP.LT.0.OR.IXP.GT.1023.OR.IYP.LT.0.OR.IYP.GT.780) GOTO 500
      XP=IXP
      YP=IYP
450   CALL PLOTC(XP,YP,1,PHYS,ID,1,1,1)
500   IX1=IX+1
      IY1=IY+1
      IF(IX1.GT.NX.OR.IY1.GT.NY.OR.IX.LT.1) GOTO 1100
      NIN=0
      NON=0
510   IOY=IY
520   IOX=IX
C
C     FIND POTENTIALS OF 4 POINTS SURROUNDING ION.
600   DO 850 J=IY,IY1
610   DO 800 I=IX,IX1
      K=I+(J-1)*NX
      NIN=NIN+1
      P(NIN)=A(K)
C
C     IF POINT IS AN ELECTRODE POINT, SUBTRACT ELECT2 FROM POTENTIAL.
700   IF(P(NIN)-ELECT) 800,710,710
710   P(NIN)=P(NIN)-ELECT2
      NON=NON+1
      IF(NOM.EQ.3) ASSIGN 1100 TO IPOTL
C
C     HITS ELECTRODE.
800   CONTINUE
850   CONTINUE
860   DSX=X0-IX
      DSY=Y0-IY
      P(5)=P(1)+DSX*(P(2)-P(1))
      P(6)=P(3)+DSX*(P(4)-P(3))
      P(7)=P(1)+DSY*(P(3)-P(1))
      P(8)=P(2)+DSY*(P(4)-P(2))
C
C     CALC POTENTIAL GRADIENTS >FORCES >NEW VELOCITIES >NEW POSITION.
900   FX=P(7)-P(8)
      FY=P(5)-P(6)
      IF(Y0.LT.2.0.AND.KCYL.GE.0) FY=(FY+FY)*(Y0-1.0)
905   VXN=VX0 + FX*FM*FAC(IFR)
      VYN=VY0 + FY*FM*FAC(IFR)
910   X0 = X0 + (VX0+VXN)*T2
      Y0 = Y0 + (VY0+VYN)*T2
      VY0=VYN
      VX0=VXN
      GOTO IPOTL
920   ASSIGN 950 TO IPOTL
C
```

```
C     CALCULATE POTENTIAL AT STARTING COORDINATES.
930   STAPOT=VSCALE*(P(5)+DSY*(P(6)-P(5)))*FAC(IFR)
950   CONTINUE
1000  CONTINUE
      IFR=1
C
C     DRAW FINAL SEGMENT OF TRAJECTORY.
1100  IXP=SCALE*(X0-1.0)
      IYP=YSCALE*(Y0-1.0)
      IF(IXP.LT.0.OR.IXP.GT.1023.OR.IYP.LT.0.OR.IYP.GT.780) GOTO 1200
      XP=IXP
      YP=IYP
1150  CALL PLOTC(XP,YP,1,PHYS,ID,1,1,1)
C
C     CALCULATE POTENTIAL AT FINAL COORDINATES.
1200  POTL=VSCALE*FAC(IFR)*(P(5)+DSY*(P(6)-P(5)))
      DST=GS*SQRT(ABS((X0-35.5)**2+(Y0-35.5)**2))
      ENERGY=0.5*(VX0*VX0+VY0*VY0)*EMASS
      ANGLE =ATAN(VY0/VX0)
      ANGLE =ANGLE*180.0/3.1415926
      IF(VY0.LT.0.0) ANGLE=ANGLE-180.0
C
C     CALCULATE ERROR BY CONSERVATION OF ENERGY.
1300  ERROR=ABS(POTL-STAPOT)-ABS(SEN-ENERGY-ELOSS)
      IF(TOF.GT.TNP) GO TO 1305
      WRITE(5,*)'UNSTABLE'
      GO TO 1310
1305  IF(ORF.GT.BST) GO TO 1306
      WRITE(5,*)'STABLE'
      GO TO 1310
1306  WRITE(5,*)'PASS'
1310  WRITE(5,1311) X0,Y0,ENERGY,ANGLE
1311  FORMAT(' FINAL   X=',F8.2,4X,'Y=',F8.2,4X,'ENERGY=',F10.2,
     14X,'ANGLE=',F8.2)
      WRITE(5,1312) ERROR,TNP,TOF
1312  FORMAT(' ERROR=',F10.2,4X,'TNP=',F10.4,4X,'TOF=',F10.4,
     1' MICROSECONDS.')
1400  CONTINUE
1450  CALL PLOTC(XP,YP,1,PHYS,ID,1,-1,0)
1500  RETURN
      END
```

```
      SUBROUTINE PLOTC (XA,YA,NPNT,PHYS,IDDEV,IMODE,INIT,IDF)
C
C=====================================================================
C
C     TITLE:  PLOTC.FTN - SIMPLE ARRAY PLOTTER
C
C     AUTHOR:  T V ATKINSON
C              DEPARTMENT OF CHEMISTRY
C              MICHIGAN STATE UNIVERSITY
C              EAST LANSING, MI 48824
C
C     DATE:  17-APR-80
C
C---------------------------------------------------------------------
C
C     ARGUMENT LIST:
C
C          XA       REAL ARRAY CONTAINING THE X-COORDINATE OF THE
C                           POINTS TO BE PLOTTED
C
C          YA       REAL ARRAY CONTAINING THE Y-COORDINATE OF THE
C                           POINTS TO BE PLOTTED
C
C          NPNT     NUMBER OF POINTS TO BE PLOTTED
C
C          PHYS     PLOT SURFACE DEFINITIONS
C                    (1) X MARGIN (PHYSICAL UNITS)
C                    (2) X-AXIS LENGTH
C                    (3) Y-MARGIN
C                    (4) Y-AXIS LENGTH
C
C                           (THE FOLLOWING APPLY FOR IMODE = 1)
C                    (5) XMIN
C                    (6) XMAX
C                    (7) YMIN
C                    (8) YMAX
C
C          IDDEV    DEVICE NUMBER
C                   =0 VECTOR LIST INTO FILE
C                   =1 TEKTRONIX 4010 TERMINAL
C                   =2 VERSATEC
C                   =3 PRINTRONIX
C
C          IMODE    EXTREMA CONTROL
C                   =0 PLOT SEARCHES FOR EXTREMA
C                   =1 USER SUPPLIES EXTREMA
C
C          INIT     INITIATION CONDITION
C                   =-1 TERMINATE PLOT AFTER THIS PLOT
C                   = 0 NEW PLOT
C                   = 1 CONTINUE WITH SAME VALUES
C
C          IDF      DRAW FACTOR
C                   =-1 MOVE THE CURSOR, NO PLOT
C                   = 0 PLOT DOTS
C                   = 1 PLOT LINE
C
C=====================================================================
C
```

```
C
C=====================================================================
C
C=====================================================================
C
C       MODIFIED BY:  JIIN-WU CHAI, DEPT. OF CHEM., NSU, 20-AUG-80
C
C=====================================================================
C
C       VECTOR.COM
C
C=====================================================================
C
        COMMON/VECTOR/XSCALE,YSCALE,IDEV,TRNFRM(6),SCAL
        COMMON/VOLAY/XOFFC,YOFFC,XLC,YLC,XV(10),YV(10),NI
        COMMON/OFILE/LUNVLT,LUNTIV
        COMMON/VTEK/XUPPER,YUPPER,NIBS,LINPAT
C
C=====================================================================
C
C       PLOTC.FTN
C
C=====================================================================
C
        DIMENSION XA(1),YA(1),PHYS(8)
C
        IF(INIT) 160,1,120
 1      NIBS = 1
        LINPAT = -1
        IDEV = IDDEV
        LUNVLT = 1
        LUNTIV = 5
        DO 10 I=1,6
 10     TRNFRM(I) = 0.0
        TRNFRM(1) = 1.0
        TRNFRM(5) = 1.0
        RMAX = 1.0E37
C
C       USE USER'S EXTREMA
C
        IF (INODE.EQ.0) GO TO 50
        XMIN = PHYS(5)
        XMAX = PHYS(6)
        YMIN = PHYS(7)
        YMAX = PHYS(8)
        GO TO 110
C
C       FIND EXTREMA
C
 50     XMAX = -RMAX
        XMIN =  RMAX
        YMAX = -RMAX
        YMIN =  RMAX
        DO 100 I=1,NPNT
        X = XA(I)
        Y = YA(I)
        XMAX = AMAX1(X,XMAX)
        XMIN = AMIN1(X,XMIN)
        YMAX = AMAX1(Y,YMAX)
 100    YMIN = AMIN1(Y,YMIN)
```

```
C
C       SET UP PLOTTING SURFACE
C
 110    WRITE (5,8900) XMIN,XMAX,YMIN,YMAX
 8900   FORMAT (' PLOT-EXTREMA: ',4E15.6)
        XSCALE = (XMAX - XMIN)/PHYS(2)
        YSCALE = (YMAX - YMIN)/PHYS(4)
        XUPPER = 2.0*PHYS(1) + PHYS(2)
        YUPPER = 2.0*PHYS(3) + PHYS(4)
        CALL VECTOR (0.0,0.0,0)
        XOFFC = PHYS(1) - XMIN/XSCALE
        YOFFC = PHYS(3) - YMIN/YSCALE
C
C       DRAW A BOX AROUND THE PLOTTING SURFACE
C
        CALL VECTOR (XMIN,YMIN,1)
        CALL VECTOR (XMIN,YMAX,2)
        CALL VECTOR (XMAX,YMAX,2)
        CALL VECTOR (XMAX,YMIN,2)
        CALL VECTOR (XMIN,YMIN,2)
C
C       DRAW THE ARRAY
C
 120    IF(IDF) 130,140,150
 130    CALL VECTOR(XA,YA,1)
        GOTO 170
 140    CALL VECTOR(XA,YA,1)
        CALL VECTOR(XA,YA,2)
        GOTO 170
 150    CALL VECTOR(XA,YA,2)
        GOTO 170
 160    CALL VECTOR(XA,YA,4)
 170    RETURN
        END
```

```
C       PROGRAM TABLE.FTN
C
        DIMENSION FAC(100)
        DOUBLE PRECISION PI,TPI,FPI,HPI,X,FNORM
        CALL ASSIGN(5,'TI:')
        CALL ASSIGN(6,'LP:')
        PI=3.14159265358979320
        TPI=PI/2.0D0
        FPI=PI/50.0D0
        HPI=PI/100.0D0
        FNORM=1.0D0/(DCOS(TPI+HPI)-DCOS(TPI-HPI))
        X=0.0D0
        TFAC=0.0
        WRITE(5,10)
10      FORMAT('1PROGRAM TABLE.FTN')
        WRITE(5,20)
20      FORMAT(//8X,' SINE',15X,' FAC(I)',13X,' TFAC')
        DO 100 I=1,100
        FAC(I)=FNORM*(DCOS(X+HPI)-DCOS(X-HPI))
        SINE=DSIN(X)
        X=X+FPI
        TFAC=TFAC+FAC(I)
        WRITE(5,30) SINE,FAC(I),TFAC
30      FORMAT(3G20.10)
100     CONTINUE
        FAC(100)=0.0-TFAC
        CALL ASSIGN(2,'QTABLE.BIN')
        WRITE(2) (FAC(I),I=1,100)
        CALL CLOSE(2)
        PAUSE 'QTABLE.BIN FINISHED'
        CALL EXIT
        END
```

REFERENCES

REFERENCES

1. R.A.Yost and C.G.Enke, J. Am. Chem. Soc., 100 (1978) 2274.

2. R.A.Yost and C.G.Enke, Anal. Chem., 50 (1979) 1251A.

3. "An Automated Triple Quadrupole Mass Spectrometer", H.R. Gregg, J.W.Chai, J.A.Chakel, P.A.Hoffman, R.K.Latven, R.S.Matthews, C.A.Myerholtz, B.H.Newcome, and C.G.Enke, 29th Annual Conference on Mass Spectrometry and Allied Topics, Minneapolis, MN, May 24-29, 1981.

4. R.A.Yost and C.G.Enke, Int. J. Mass Spectrom. Ion Phys., 30 (1979) 127.

5. R.A.Yost and C.G.Enke, Org. Mass Spectrom. 16 (1981) 171.

6. P.H.Dawson, Quadrupole Mass Spectrometry and Its Applications, Elsevier, New York, 1976.

7. P.H.Dawson and M.Meunier, Int. J. Mass Spectrom. Ion Phys., 29 (1979) 269.

8. D.C.McGilvery and J.D.Morrison, ibid, 28 (1978) 81.

9. P.K.Ghosh and A.S.Arora, ibid, 21 (1976) 343.

10. J.E.Campana and P.C.Jurs, ibid, 33 (1980) 119.

11. P.H.Dawson, ibid, 20 (1976) 237.

12. P.H.Dawson, ibid, 36 (1980) 353.

13. A.S.Arora, A.Agarwal and P.K.Ghosh, ibid, 24 (1977) 1.

14. R.F.Bonner, G.F.Hamilton, and R.E.March, ibid, 30 (1979) 365.

15. J.A.Richards and R.N.McLellan, ibid, 17 (1975) 17.

16. P.H.Dawson, ibid, 25 (1977) 375.

17. P.H.Dawson, ibid, 21 (1976) 317.

18. J.F.Hennequin and R.L.Inglebert, ibid, 26 (1978) 131.

19. Digital Equipment Corporation. Maynard, Massachusetts.

20. W.Fock, Int. J. Mass Spectrom. Ion Phys., 3 (1969) 285.

21. S.Beg and N.A.Malik, ibid, 27 (1978) 49.

22. G.Conforti, F.D.Giallo, F.Pieralli, G.Ventura, and G.Zaccanti, ibid, 36 (1980) 343.

23. S.L.Koontz and M.B.Denton, ibid, 37 (1981) 227.

24. J.Michnowicz and B.Munson, Org. Mass Spectro., 4 (1970) 481.

25. D.Beggs, M.L.Vestal, H.M.Fales, and G.W.A.Milne, Rev. Sci. Instrum., 42 (1971) 1578.

26. C.Chang, G.J.Sroka and G.G.Meisels, Int. J. Mass Spectrom. Ion Phys., 11 (1973) 367.

27. B.Hoegger and P.Bommer, ibid, 13 (1974) 35.

28. D.F.Hunt, C.N.McEwen, and T.M.Harvey, Anal. Chem., 70 (1975) 1730.

29. H.Kambara and I.Kanomata, Int. J. Mass Spectrom. Ion Phys., 24 (1977) 453.

30. R.E.Mather and J.E.J.Todd, ibid, 30 (1979) 1.

31. A.M.Hogg and J.D.Payzant, ibid, 27 (1978) 291.

32. C.F.Giese, Rev. Sci. Instrum., 30 (1959) 260.

33. C.S.Lu and H.E.Carr, ibid, 33 (1962) 823.

34. A.J.Loveless and R.D.Russell, Int. J. Mass Spectrom. Ion Phys., 3 (1969) 257.

35. H.U.Winkler and H.D.Beckey, ibid, 39 (1981) 111.

36. F,H.Read, A.Adams and J.R.Soto-Montiel, J. Phys. E. 4 (1971) 625.

37. S.Natali, D.D.Chio, E.Uva, and C.E.Kuyatt, Rev. Sci. Instrum., 43 (1972) 80.

38. C.E.Kuyatt, S.Natali, and D.D.Chio, ibid, 43 (1972) 84.

39. J.Fink and E.Kisker, ibid, 51 (1980) 918.

40. E.Kisker, ibid, 53 (1982) 114.